
ATTENTION MECHANISMS DON'T LEARN ADDITIVE MODELS: RETHINKING FEATURE IMPORTANCE FOR TRANSFORMERS

Tobias Leemann
University of Tübingen
Technical University of Munich
tobias.leemann@uni-tuebingen.de

Alina Fastowski
Technical University of Munich
alina.fastowski@tum.de

Felix Pfeiffer
University of Tübingen
f.pfeiffer@student.uni-tuebingen.de

Gjergji Kasneci
Technical University of Munich
gjergji.kasneci@tum.de

ABSTRACT

We address the critical challenge of applying feature attribution methods to the transformer architecture, which dominates current applications in natural language processing and beyond. Traditional attribution methods to explainable AI (XAI) explicitly or implicitly rely on linear or additive surrogate models to quantify the impact of input features on a model's output. In this work, we formally prove an alarming incompatibility: transformers are structurally incapable to align with popular surrogate models for feature attribution, undermining the grounding of these conventional explanation methodologies. To address this discrepancy, we introduce the Softmax-Linked Additive Log-Odds Model (SLALOM), a novel surrogate model specifically designed to align with the transformer framework. Unlike existing methods, SLALOM demonstrates the capacity to deliver a range of faithful and insightful explanations across both synthetic and real-world datasets. Showing that diverse explanations computed from SLALOM outperform common surrogate explanations on different tasks, we highlight the need for task-specific feature attributions rather than a one-size-fits-all approach.

1 Introduction

The transformer architecture [55] has been established as the status quo in modern natural language processing [15, 38, 39, 54]. However, the current and foreseeable adoption of large language models (LLMs) in critical domains such as the judicial system [11] and the medical domain [26] comes with an increased need for transparency and interpretability. Methods to enhance the interpretability of an artificial intelligence (AI) system are developed in the research area of Explainable AI (XAI, 2, 20, 36, 9). A recent meta-study [42] shows that XAI has the potential to increase users' understanding of AI systems and their trust therein. Feature attribution methods that quantify the contribution of each input to a decision outcome are among the most popular explanation methods, and a variety of approaches have been suggested for the task of computing such attributions [27, 40, 51, 31, 14, 34].

However, it remains hard to formally define the contribution of an input feature for non-linear functions. Recent work [22] has shown that many common explanation methods do so by implicitly or explicitly performing a local approximation of the complex black-box function, denoted as f , using a simpler surrogate function g from a predefined class \mathcal{G} . For instance, Local Interpretable Model-agnostic Explanations (LIME, 40) or input gradient explanations [5] use a linear surrogate model to approximate the black-box f . An important implication of this view is the *recovery property*. This property implies that if the black-box function is already within the function class \mathcal{G} , we can effectively reconstruct the original function f from the explanations. As an example, suppose that the black box function we consider is of linear form, i.e., $f(\mathbf{x}) = \mathbf{w}^\top \mathbf{x}$. In this case, a gradient explanation as well as continuous LIME (C-LIME, 3) will recover the original model's parameters up to an offset [22, Theorem 1]. Shapley value explanations [31] possess a comparable relationship: It is known that they correspond to the feature contributions of Generalized Additive Models (GAM, 7).

Input sequence t (positive: $[0.5, \infty]$): <div style="border: 1px solid black; padding: 2px; display: inline-block;"> this is a fantastic movie . </div>	$f(t)$: BERT 1.09 linear 0.93	Common Surrogate Models in XAI <table border="1" style="width: 100%; border-collapse: collapse;"> <thead> <tr> <th>Predictive Models</th> <th>Surrogate Models</th> <th>Explanation Techniques</th> </tr> </thead> <tbody> <tr> <td>Logistic / Linear Regression, ReLU networks</td> <td>Linear Model: \timesno non-linearities \timesno interactions</td> <td>C-LIME, Gradients, IG</td> </tr> <tr> <td>GAM, ensembles, boosting</td> <td>GAM: \checkmarknon-linearities \timesno interactions</td> <td>Removal-based, e.g. Shapley Values, Local GAM approx.</td> </tr> <tr> <td>Transformers</td> <td>SLALOM (ours): \checkmarknon-linearities \checkmarkinteractions</td> <td>Local SLALOM approx.</td> </tr> </tbody> </table>	Predictive Models	Surrogate Models	Explanation Techniques	Logistic / Linear Regression, ReLU networks	Linear Model: \times no non-linearities \times no interactions	C-LIME, Gradients, IG	GAM, ensembles, boosting	GAM: \checkmark non-linearities \times no interactions	Removal-based, e.g. Shapley Values, Local GAM approx.	Transformers	SLALOM (ours): \checkmark non-linearities \checkmark interactions	Local SLALOM approx.
Predictive Models	Surrogate Models		Explanation Techniques											
Logistic / Linear Regression, ReLU networks	Linear Model: \times no non-linearities \times no interactions		C-LIME, Gradients, IG											
GAM, ensembles, boosting	GAM: \checkmark non-linearities \times no interactions		Removal-based, e.g. Shapley Values, Local GAM approx.											
Transformers	SLALOM (ours): \checkmark non-linearities \checkmark interactions	Local SLALOM approx.												
Add prefix u (neutral: $[-0.5, 0.5]$): <div style="border: 1px solid black; padding: 2px; display: inline-block;"> it has been a long time since we saw the last movie because something always happened to come up . however . </div>	$f(u)$: BERT 0.29 linear 0.19													
Concatenation $[t, u]$: <div style="border: 1px solid black; padding: 2px; display: inline-block;"> it has been a long time since we saw the last movie because something always happened to come up . however . this is a fantastic movie . </div>	$f(t) + f(u)$: Σ BERT 1.38 Σ linear 1.12													
$f([t, u])$: BERT 0.45 linear 1.12														

Figure 1: **Transformers cannot be well explained through additive models.** Left: We exemplarily show the log-odds for the outputs of a BERT model and a linear Naïve-Bayes model (“linear”) trained on the IMDB movie review dataset. We pass two sequences to the model independently and in concatenation. While for the linear model, the output of the concatenated sequence can be described by the sum, this is not the case for BERT. We show that this phenomenon is not due to a non-linearity in this particular model but stems from a general incapacity of transformers to represent additive functions. Right: To overcome this difficulty, we propose SLALOM, a novel surrogate model specifically designed to better approximate transformer models.

The significance of recovery properties lies in their role when explanations are leveraged to gain insights into the underlying data. Particularly in applications like XAI for scientific discovery, preserving the path from the input data to the explanation through a learned model is crucial. These guarantees, however, hold practical value only when the black-box model can be approximated by the chosen surrogate function class \mathcal{G} at least within some local region.

In this study, we demonstrate that the transformer architecture, the main building block of LLMs such as the GPT models [39], is inherently incapable of learning additive and linear models on the input tokens, both theoretically and empirically. We formally prove that encoder-only and decoder-only transformers structurally cannot represent additive models due to the attention mechanism’s softmax normalization, which necessarily introduces token dependencies over the entire sequence length. An example is illustrated in Figure 1 (left).

Our findings imply that additive explanations *cannot* be faithful to transformers. This is a significant oversight in current XAI practices which undermines the explanations’ recovery properties. As our results suggest that the role of tokens cannot be described through a single score, we introduce the Softmax-Linked Additive Log-Odds Model (SLALOM, cf. Figure 1, right), which represents the role of each input token in two dimensions: The *token value* describes the independent effect of a token, whereas the *token importance* provides a token’s interaction weight when combined with other tokens in a sequence. In summary, our work offers the following contributions over the related literature:

- (1) We theoretically and empirically demonstrate that common transformer architectures fail to represent GAMs and linear models on the input tokens, reducing explanation faithfulness
- (2) To mitigate these issues, we propose the Softmax-Linked Additive Log-Odds Model (SLALOM), which uses a combination of two scores to quantify the role of input tokens
- (3) We theoretically analyze SLALOM and show that (i) it can be represented by transformers, (ii) it can be uniquely identified from data, and (iii) it is highly efficient to estimate
- (4) Experiments on synthetic and real-world datasets with common language models (LMs) confirm the mismatch between surrogate models and predictive models and underline that single scores like LIME [40] or SHAP [31] do not cover different angles of interpretability, such as human attention or faithfulness metrics, as precisely as scores by SLALOM

2 Related Work

Explainability for Transformers. Various methods exist to tackle model explainability [36, 9]. Furthermore, specific approaches have been devised for the transformer architecture [55]: As the attention mechanism at the heart of transformer models is supposed to focus on relevant tokens, it seems a good target for explainability methods. Several works are turning to attention patterns as model explanation techniques. A central attention-based method is put forward by Abnar and Zuidema [1], who propose two methods of aggregating raw attentions across layers, *flow* and

rollout. Brunner et al. [8] focus on effective attentions, which aim to identify the portion of attention weights actually influencing the model’s decision. While these approaches follow a scalar approach considering only attention weights, Kobayashi et al. [28, 29] propose a norm-based vector-valued analysis, arguing that relying solely on attention weights is insufficient and the other components of the model need to be considered. Building on the norm-based approach, Modarressi et al. [34, 35] further follow down the path of decomposing the transformer architecture, presenting global level explanations with the help of rollout. Beyond that, many more attention-based explanation approaches have been put forward [12, 23, 18, 37, 50, 58]. However, it is debatable whether attention scores are suitable for explainability [56, 25, 46]. Despite the active research in the area, the recovery property is not considered in these prior works and their scope is often limited to very specific transformer models.

Model-agnostic XAI. Researchers have therefore devised model-agnostic explanations that can be applied without precise knowledge of a model’s architecture. Model-agnostic local explanations like LIME [40], SHAP [31] and others [47, 51, 49, 57, 14, etc.] are a particularly popular class of explanations that are applied to LMs as well [52, 44, 17]. Surrogate models are a common subform [22], which locally approximate a black-box model through a simple, interpretable function.

Linking Models and Explanations. Prior work has distilled the link between classes of surrogate models that can be recovered by explanations [3, 22, Theorem 3]. Notable works include Garreau and von Luxburg [19] which provides analytical results on different parametrizations of LIME and Bordt and von Luxburg [7] which formalizes the connection between Shapley values and GAMs for classical Shapley values as well as n -Shapley values that can also model higher-order interactions. We contribute to the literature by showing that transformers are inherently incapable to represent GAMs or linear models, casting doubts on the applicability of LIME and SHAP to transformers. We provide SLALOM, a novel surrogate model that maintains a recovery property for transformers.

3 Preliminaries

3.1 Input and output representations

In this work, we focus on classification problems of token sequences. For the sake of simplicity, we initially consider a 2-class classification problem with labels $y \in \mathcal{Y} = \{0, 1\}$. We will outline how to generalize our approaches to multi-class problems in Appendix C.1.

The input consists of a sequence of tokens $t = [t_1, \dots, t_{|t|}]$ where $|t| \in 1, \dots, C$ is the sequence length that can span at most C tokens (the context length). The tokens stem from a finite size vocabulary \mathcal{V} , i.e., $t_i \in \mathcal{V}, i = 1, \dots, |t|$. To transform the tokens into a representation amenable to processing with computational methods, the tokens need to be encoded as numerical vectors. To this end, an embedding function $e : \mathcal{V} \rightarrow \mathbb{R}^d$ is used, where d is the embedding dimension. Let $e_i = e(t_i)$ be the embedding of the i -th token such that the entire sentence is embedded in a matrix $E = [e_1, \dots, e_{|t|}]^T \in \mathbb{R}^{|t| \times d}$. The output is given by a logit vector $l \in \mathbb{R}^{|\mathcal{Y}|}$, such that $\text{softmax}(l)$ contains individual class probabilities.

3.2 The common transformer architecture

Many popular LMs follow the transformer architecture introduced by Vaswani et al. [55] with only minor modifications. We will introduce the most relevant building blocks of the architecture in this section. A complete formalization is given in Appendix B.1. A schematic overview of the architecture is visualized in Figure 2. Let us denote the input embedding of token $i = 1, \dots, |t|$ in layer $l \in 1, \dots, L$ by $h_i^{(l-1)} \in \mathbb{R}^d$, where $h_i^{(0)} = e_i$. The core component of the attention architecture is the attention head. Although we only formalize a single head here, our theoretical results cover multiple heads. For each token, a *query*, *key*, and a *value* vector are computed by applying an affine-linear transform to the input embeddings. Keys and queries are projected onto each other and normalized by a row-wise softmax operation resulting in attention weights $\alpha_{ij} \in [0, 1]$, denoting how much token i is influenced by token j . The attention output for token i can be computed as $s_i = \sum_{j=1}^{|t|} \alpha_{ij} v_j$, where $v_j \in \mathbb{R}^{d_h}$ denotes the value vector for token j . The final s_i are

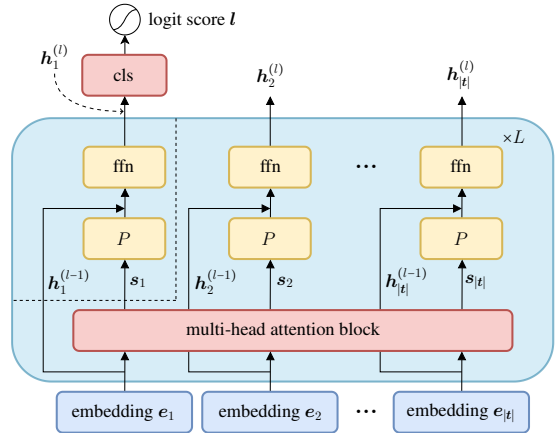


Figure 2: **Transformer architecture.** In each layer, input embeddings $h_i^{(l-1)}$ for each token i are transformed into output embeddings $h_i^{(l)}$. When detaching the part prior to the classification head (“cls”), we see that the output only depends on the last embedding $h_1^{(l-1)}$ and attention output s_1 .

projected back to dimension d by a projection operator $P : \mathbb{R}^{d_h} \rightarrow \mathbb{R}^d$ before they are added to the corresponding input embedding $\mathbf{h}_i^{(l-1)}$ as mandated by skip-connections. The sum is then transformed by a nonlinear function that we denote by $\text{ffn} : \mathbb{R}^d \rightarrow \mathbb{R}^d$, finally resulting in a transformed embedding $\mathbf{h}_i^{(l)}$. This procedure is repeated iteratively for layers $1, \dots, L$ such that we finally arrive at output embeddings $\mathbf{h}_i^{(L)}$. To perform classification, a classification head $\text{cls} : \mathbb{R}^d \rightarrow \mathbb{R}^{|\mathcal{Y}|}$ is put on top of a token at some index r (how this token is chosen depends on the architecture, common choices include $r \in \{1, |\mathbf{t}|\}$), such that we get the final logit output $\mathbf{l} = \text{cls}(\mathbf{h}_r^{(L)})$. The logit output is transformed to a probability vector via another softmax operation. Note that in the two-class case, we obtain the log-odds $F(\mathbf{t})$ by taking the difference (Δ) between the two logits, i.e., $F(\mathbf{t}) := \log \frac{p(y=1|\mathbf{t})}{p(y=0|\mathbf{t})} = \Delta(\mathbf{l}) = \mathbf{l}_1 - \mathbf{l}_0$.

3.3 Encoder-Only and Decoder-Only models

Practical implementations introduce subtle modifications into the process described previously. The most relevant distinction is made between *encoder-only* models, that include BERT [15] and its variants, and *decoder-only* models such as the GPT models [38, 39].

Encoder-only models. Considering BERT as an example of an encoder-only model, the first token is used for the classification, i.e., $r = 1$. Usually, a special token [CLS] is prepended to the text at position 1, however this is not strictly necessary for the functioning of the model.

Decoder-only models. In contrast, decoder-models like GPT-2 [39] add the classification head on top of the last token for classification, i.e., $r = |\mathbf{t}|$. A key difference is that in GPT-2 and other decoder-only models, a causal mask is laid over the attention matrix, resulting in $\alpha_{i,j} = 0$ for $j > i$. This encodes the constraint that tokens can only attend to themselves or to previous ones.

4 Analysis

Let us initially consider a transformer with only a single layer and head. Our first insight is that the classification output can be determined only by two values: the input embedding at the classification token r , $\mathbf{h}_r^{(0)}$, and the attention output s_r . This can be seen when plugging in the different steps:

$$F(\mathbf{t}) = \Delta(\text{cls}(\mathbf{h}_r^{(1)})) = \Delta(\text{cls}(\text{ffn}(\mathbf{h}_r^{(0)} + \mathbf{P}(s_r)))) = g(\mathbf{h}_r^{(0)}, s_r) = g\left(\mathbf{h}_r^{(0)}, \sum_{j=1}^{|\mathbf{t}|} a_{rj} \mathbf{v}_j\right). \quad (1)$$

Note that at this point, we can let the sum go towards $|\mathbf{t}|$ for both encoder and decoder models. For encoder models, this is the default. For decoder models, we have $s_r = \sum_{j=1}^r a_{rj} \mathbf{v}_j$ but as $r = |\mathbf{t}|$, the outcome is the same as given in Eqn. (1).

4.1 Transformers cannot represent additive models

We now consider how this architecture would represent a linear model. In this model, each token is assigned a weight $w : \mathcal{V} \rightarrow \mathbb{R}$. The output obtained by adding weights and an offset $b \in \mathbb{R}$:

$$F([t_1, t_2, \dots, t_{|\mathbf{t}|}]) \stackrel{!}{=} b + \sum_{i=1}^{|\mathbf{t}|} w(t_i). \quad (2)$$

The transformer gives rise to an interesting observation when considering token sequences of identical tokens but of different lengths, i.e., $[\tau], [\tau, \tau]$, etc. We first note that the sum of the attention scores is bound to be $\sum_{j=1}^{|\mathbf{t}|} a_{rj} = 1$. The output of the attention head will thus be a weighted average of the value vectors \mathbf{v}_j . As the value vectors $\mathbf{v}_j(t_j)$ are determined purely by the input tokens t_j , for a sequence of identical tokens, we will have the same value vectors, resulting in identical vectors being averaged. In summary, this renders the transformer incapable to differentiate between sequences of different lengths. We are now ready to state our main result, which formalizes this intuition.

Proposition 4.1 (Single-layer transformers cannot represent generalized additive models (GAMs)). *Let \mathcal{V} be a vocabulary and $C \geq 2, C \in \mathbb{N}$ be a maximum sequence length (context length). Let $w_i : \mathcal{V} \rightarrow \mathbb{R}, \forall i \in 1, \dots, C$ be any mapping that assigns a token encountered at position i a numerical score including at least one token $\tau \in \mathcal{V}$ with non-zero weight $w_i(\tau) \neq 0$ for some $i \in 2, \dots, C$. Let $b \in \mathbb{R}$ be an arbitrary offset. Then, there exists no parametrization of the encoder or decoder single-layer transformer F such that for every sequence $\mathbf{t} = [t_1, t_2, \dots, t_{|\mathbf{t}|}]$ with length $|\mathbf{t}| \leq C$, the output of the transformer network is equivalent to $F([t_1, t_2, \dots, t_{|\mathbf{t}|}]) = b + \sum_{i=1}^{|\mathbf{t}|} w_i(t_i)$.*

Proof Sketch. We prove the statement by concatenating the token τ to sequences of different length. We then show that the inputs to the final part g of the transformer will be independent of the sequence length. Due to g being deterministic, the output will also be independent of the sequence length. This is contradictory to the GAM model with a weight $w_j(\tau) \neq 0$ requiring different outputs for sequences of length $j-1$ and j . Formal proofs for all results can be found in Appendix B. \square

In simple terms, the proposition states that the transformer cannot represent GAMs for sequences of more than one token apart from trivial constant functions. Importantly, the class of functions stated in the above theorem includes the prominent case of linear models in Eqn. (1), where each token has a certain weight w independent of its position in the input vector (i.e., $w_i \equiv w, \forall i$, see Corollary B.2).

4.2 Transformer networks with multiple layers

In this section, we will show how the argument can be extended to multi-layer transformer networks. Denote by $\mathbf{h}_i^{(l-1)}$ the input embedding of the i th token at the l th layer. The output is governed by the recursive relation

$$\mathbf{h}_i^{(l)} = \text{ffn}_l(\mathbf{h}_i^{(l-1)} + \mathbf{P}_l(\mathbf{s}_i)) = g_l(\mathbf{h}_i^{(l-1)}, \mathbf{s}_i). \quad (3)$$

Exploiting the similar form allows us to generalize the main results to more layers recursively.

Corollary 4.2 (Multi-Layer transformers cannot learn linear models either). *Under the same conditions as in Proposition 4.1, a stack of multiple transformer blocks as in the model F neither has a parametrization sufficient to represent the linear model.*

Proof Sketch. To see this, we first prove that for identical input embeddings $\mathbf{H}^{(l-1)}$, that do not change for varying sequence lengths (although their number changes), the outputs $\mathbf{H}^{(l)}$ will be identical as well and independent of the sequence length. Subsequently, we show that the final embeddings will also be independent of the sequence length, resulting in a contradiction as before. \square

4.3 Practical Considerations

The above derivation contains two slight deviation from the transformer architecture deployed in practice, that are of minor importance for the validity of our results. First, common models such as BERT use a special token referred to as CLS-token where the classification head is placed on. In the example presented in the proof, the sequences have to be extended by this token as in $\mathbf{t}_A = [t_{\text{CLS}}, \tau]$ and $\mathbf{t}_B = [t_{\text{CLS}}, \tau, \tau]$. Thus, a small part of the attention will reside on this token as well.

To represent token order, common architectures use positional embeddings, tying the embedding vectors to the token position i . The behavior that we show in this work’s analysis does however also govern transformers with positional embeddings for the following reason: While the positional embeddings could be used by the non-linear ffn part to differentiate sequences of different length in theory, our proofs show that to represent the linear model, the softmax operation must be inverted for any input sequence. This is highly nonlinear operation and the number of possible sequences grows exponentially at a rate of $|\mathcal{V}|^C$ with the context length C . Learning-theoretic considerations (e.g., 6) show that the number of input-output pairs the two-layer networks deployed can maximally represent is bounded by $\mathcal{O}(dn_{\text{hidden}} \log(dn_{\text{hidden}}))$, which is small ($d=786, n_{\text{hidden}}=3072$ for BERT) in contrast to the number of sequences ($C = 1024, |\mathcal{V}| \approx 3 \times 10^4$). We conclude that the inversion is therefore impossible for realistic setups and positional embeddings can be neglected, which is confirmed by our empirical findings.

5 A Surrogate Model for Transformers

In the previous section, we theoretically established that transformer models struggle to represent additive functions. Note that this must not necessarily be considered a weakness. However, it certainly casts doubts on the suitability of additive models as surrogate models for explanations of transformers. For a principled approach, we consider the following four requirements to be of importance:

- (1) **Interpretability.** The surrogate model’s parameters should be inherently interpretable.
- (2) **Learnability.** The surrogate model should be easily representable by common transformers.
- (3) **Recovery.** If the predictive model falls into the surrogate model’s class, the fitted surrogate model’s parameters should match those of the predictive model.
- (4) **Efficiency.** The surrogate model should be efficient to estimate even for larger models.

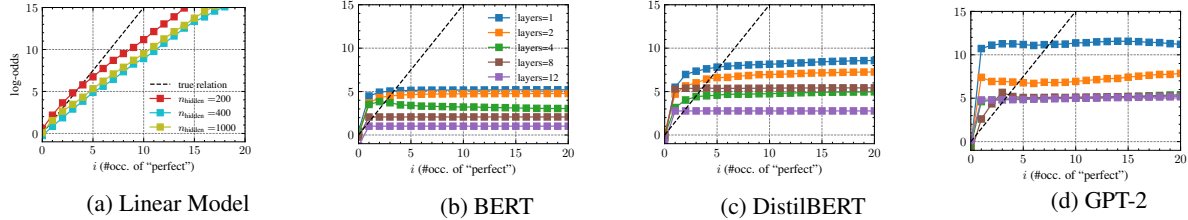


Figure 3: **Transformers fail to learn linear models.** We train different models on a synthetically sampled dataset where the log-odds obey a linear relation to the features. Fully connected models (2-layer ReLU networks with different hidden layer widths) capture the linear form of the relationship well despite some estimation error (a). However, common transformer models fail to model this relationship and output almost constant values (b)-(d). This does not change with more layers.

5.1 The Softmax-Linked Additive Log-Odds Model

To meet the requirements, we propose a novel discriminative surrogate model that explicitly models the behavior of the softmax function. Instead of only assigning a single weight w to each token, we separate two characteristics: We introduce the *token importance* as a mapping $s : \mathcal{V} \rightarrow \mathbb{R}$ and a *token value* in form of a mapping $v : \mathcal{V} \rightarrow \mathbb{R}$. Subsequently, we consider the following discriminative model:

$$F(\mathbf{t}) = \log \frac{p(y=1|\mathbf{t})}{p(y=0|\mathbf{t})} = \sum_{\tau_i \in \mathbf{t}} \alpha_i(\mathbf{t}) v(t_i), \quad \text{where } \alpha_i(\mathbf{t}) = \frac{\exp(s(t_i))}{\sum_{t_j \in \mathbf{t}} \exp(s(t_j))}. \quad (4)$$

Due to the shift invariance of the softmax function, we observe that the mappings s and s' given by $s'(\tau) = s(\tau) + \delta$ result in the same softmax-score and thus the same log-odds model for any input \mathbf{t} . Therefore, the parameterization would not be unique. To this end, we introduce a *normalization constraint* on the sum of token importances for uniqueness. Formally, we constrain it to a user-defined constant $\gamma \in \mathbb{R}$ such that $\sum_{\tau \in \mathcal{V}} s(\tau) = \gamma$, where natural choices include $\gamma \in \{0, 1\}$. We refer to the discriminative model given in Eqn. (4) together with the normalization constraint as the *softmax-linked additive log-odds model* (SLALOM).

As common in surrogate model explanations, we can fit SLALOM to a predictive model’s outputs globally or locally and use tuples of token importance scores and token values scores, $(v(\tau), s(\tau))$ to give explanations for an input token τ . While the value score provides an absolute contribution of τ to the output, its token importance $s(\tau)$ determines its weight with respect to the other tokens. For instance, if only one token τ is present in a sequence, the output is only determined by its value score $v(\tau)$. However, in a sequence of multiple tokens, the importance of each token with respect to the others – and thereby the contribution of this token’s value – is determined by the token importance scores s . This intuitive relation makes SLALOM interpretable, thereby satisfying Property (1).

5.2 Theoretical properties of SLALOM

We analyze the proposed SLALOM theoretically to ensure that it fulfills Properties (2) and (3), Learnability and Recovery, and subsequently provide efficient algorithms to estimate its parameters (4). First, we show that – unlike linear models, SLALOMs can be easily learned by transformers.

Proposition 5.1 (Transformers can fit SLALOM). *For any mapping s, v and a transformer with an embedding size d and head dimension d_h with $d, d_h \geq 3$, there exists a parameterization of the transformer to reflect SLALOM in Equation (4) together with the normalization constraint.*

Proof Sketch. We prove this statement by explicitly constructing the weight matrices of the transformer for this mapping. In particular, this involves obtaining raw attention scores of $s(t_j)$ for key t_j that are normalized as in the SLALOM model. See the full proof for the full construction in the appendix. \square

This proposition highlights that – unlike linear models – there are simple ways for the transformer to represent relations governed by SLALOMs. We demonstrate this empirically in our experimental section and conclude that SLALOM fulfills Property (2). For Property (3), Recovery, we make the following proposition:

Proposition 5.2 (Recovery of SLALOMs). *Suppose query access to a model G that takes sequences of tokens \mathbf{t} with lengths $|\mathbf{t}| \in 1, \dots, C$ and returns the log-odds according to a non-constant SLALOM on a vocabulary \mathcal{V} , normalization constant $\tau \in \mathbb{R}$, but with unknown parameter mappings $s : \mathcal{V} \rightarrow \mathbb{R}, v : \mathcal{V} \rightarrow \mathbb{R}$. For $C \geq 2$, we can recover the true mappings s, v with $2|\mathcal{V}| - 1$ forward passes of F .*

Proof Sketch. We first query $G([\tau]), \forall \tau \in \mathcal{V}$ for single token sequences. We know that for $|t| = 1$ all attention is on one token, i.e., $(\alpha_i = 1)$ and we thus have $G([\tau]) = v(\tau)$. Having the values of each token, We then query $n - 1$ two-token sequences with $G([\tau, \omega]), \omega \in \mathcal{V} \setminus \{\tau\}$. Given the token’s value scores, we can obtain their relative importances using $n - 1$ forward passes. We use the condition that the SLALOM is non-constant to make sure $v(\tau)$ and $v(\omega)$ are always different and we can use the output to obtain the importances mapping s . \square

This statement confirms property (3) and shows that SLALOM can be uniquely reidentified when we rule out the corner case of constant models.

Complexity considerations. Computational complexity can be a concern for XAI methods. To estimate exact Shapley values, the model’s output on exponentially many feature coalitions needs to be evaluated. However, as the proof of Proposition 5.2 shows, to estimate SLALOM’s parameters for an input sequence of \mathcal{V} tokens, only $2|\mathcal{V}| - 1$ forward passes are required, verifying Property (4). We empirically show that computing SLALOM explanations is about **8× faster** than computing LIME or SHAP explanations using the same number of samples (cf. Appendix F.7 for results and details).

5.3 Numerical Algorithms for computing SLALOMs

We suggest two algorithms to fit SLALOMs post-hoc on input-output pairs of a trained model:

SLALOM-Ana. We can use the analytical solution given in the proof of Proposition 5.2. However, the algorithm is numerically unstable as it uses a small number of short sequences (cf. Appendix F.3).

SLALOM-SGD. To this end we use SGD to optimize SLALOM’s parameters such that the logit output of the transformer closely resembles that of the surrogate SLALOM on a number of query samples. To explain a specific sample, we obtained good results when fitting SLALOM on random sequences made up of its tokens (see Appendix D for pseudocode).

5.4 Relating SLALOM scores to linear attributions

Importantly, SLALOM scores can be readily converted to locally linear interpretability scores for applications where necessary. For this purpose, a differentiable model for soft removals is required. We consider the following weighted model:

$$F(\lambda) = \frac{\sum_{t_i \in t} \lambda_i \exp(s(t_i)) v(t_i)}{\sum_{t_i \in t} \lambda_i \exp(s(t_i))}, \quad (5)$$

where $\lambda_i = 1$ if a token is present and $\lambda_i = 0$ if it is absent. We observe that setting $\lambda_i = 0$ has the desired effect of making the output of the soft-removal model equivalent to that of the standard SLALOM on a sequence without this token. Taking the gradients at $\lambda = 1$ we obtain $\frac{\partial F}{\partial \lambda_i} \Big|_{\lambda=1} \propto v(t_i) \exp(s(t_i))$, which can be used to rank tokens according to the linearized attributions. We defer the derivation to Appendix B.7 and refer to these scores as *linearized* SLALOM scores.

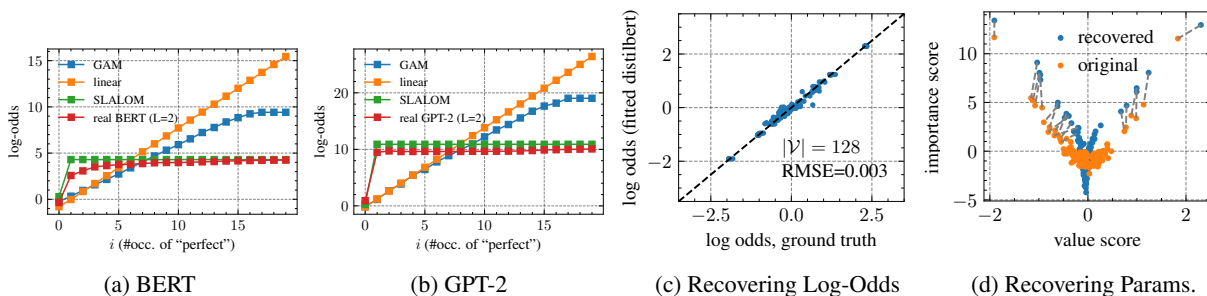


Figure 4: **SLALOM describes outputs of transformer models well (a, b).** Fitting SLALOM to the outputs of the models shown in Figure 3. Despite having $C/2=15\times$ more parameters than the SLALOM model, the GAM model does not match the transformer behavior. We provide quantitative results in Table 5 (Appendix). **Recovering SLALOMs.** We observe that we can recover the original logit-scores by fitting SLALOM on a 2-layer DistilBERT model (c) and we see a strong connection between original SLALOM parameters and the recovered ones (d). More results in Appendix F.2.

6 Experimental Evaluation

We run a series of experiments show the mismatch between surrogate model explanations and the transformers. Specifically, we verify that (1) real transformers fail to learn additive models, (2) SLALOM better captures transformer output, (3) SLALOM models can be reidentified from fitted models with tolerable error, and (4) SLALOM is more versatile than other methods as it aligns will with linear attribution scores and human attention, and performs better in faithfulness metrics. For experiments (1)-(3), we require knowledge of the ground truth, and therefore use synthetic datasets. To demonstrate the practical strengths of our method, all the experiments for (4) are conducted on real-world datasets, in comparison with state-of-the-art XAI techniques.

6.1 Experimental Setup

LM architectures. We study three representative transformer language model architectures in our experiments. In sequence classification, mid-sized transformer LMs are most common [24], which is reflected by our experimental setup. To represent the family of encoder-only models, we deploy BERT [15] and DistilBERT [43]. We further experiment with GPT-2 [39], which is a decoder-only model. We use the transformers framework to run our experiments. While not the main scope of this work, we show that SLALOM can be applied to LLMs with up to 7B parameters and non-transformer models such as Mamba [21] with plausible results due to its general expressivity in Appendix F.8.

Datasets. We use two real-world datasets for sentiment classification. Specifically, we study the IMDB dataset, consisting of movie reviews [32] and Yelp-HAT, a dataset of Yelp reviews, for which human annotators have provided annotations on which tokens are relevant for the classification outcome [45]. We provide additional details on training and datasets in Appendix E.

6.2 Evaluation with Known Ground Truth

Transformers fail to capture linear relationships. We start our experimental section by experimentally verifying the claims made in Proposition 4.1 and Corollary 4.2. To ascertain that the underlying relation captured by the models is additive, we resort to a synthetic dataset. The dataset is created as follows: First, we sample different sequence lengths from a binomial distribution with a mean of 15. Second, we sample words independently from a vocabulary of size 10. This vocabulary was chosen to include positive words, negative words, and neutral words, with manually assigned weights $w \in \{-1.5, -1, 0, 1, 1.5\}$, that can be used to compute a linear log-odds model. We evaluate this model and finally sample the sequence label accordingly, thereby ensuring a linear relation between input sequences and log-odds. We train transformer models on this dataset and evaluate them on sequences containing the same word (“perfect”) multiple times. Our results in Figure 3 show that the models fail to capture the relationship regardless of the model or number of layers used. In Appendix A, we show how this undermines the recovery property with Shapley value explanations.

Fitting SLALOM as a surrogate to transformer models. Having demonstrated the mismatch between additive functions and transformers, we turn to SLALOM as a more suitable surrogate model. As shown in Proposition 5.1, transformers can easily fit SLALOMs, which is why we hypothesize that they should model the output of such a model well in practice. We observe that this is indeed the case in Figure 4(a, b) even if the GAM has considerably more parameters than SLALOM.

Verifying Recovery. We run an experiment to study whether, unlike linear models, SLALOM can be fitted and recovered by transformers. To test this, we sample a dataset that exactly follows the distribution given by SLALOM. We then train transformer models on this dataset. The results in Figure 4(c, d) show that the surrogate model fitted on transformer outputs as a post-hoc explanation recovers the correct log-odds mandated by SLALOM (c) and that there is a good correspondence between the true model’s and the recovered model’s parameters (d).

6.3 Examining Real-World Predictions from Different Angles

We increase difficulty and deploy SLALOM to explain predictions on real-world datasets. As there is no ground truth for these datasets, it is challenging to evaluate the quality of the explanations [41]. However, we provide comparisons from several angles: We compare to linear scores obtained when fitting a Naïve-Bayes Bag-of-Words model, scores on removal and insertion benchmarks [53, 16], the human attention scores available on the Yelp-HAT dataset [45], and provide qualitative results.

Explaining Sentiment Classification. We show qualitative results for explaining a movie review in Figure 5. The figure shows that both negative and positive words are assigned high importance scores but have value scores of

LM	values v	importances s	lin.
D-BERT	0.69 ± 0.01	0.32 ± 0.02	0.70 ± 0.01
BERT	0.75 ± 0.01	0.43 ± 0.02	0.77 ± 0.01
GPT-2	0.70 ± 0.02	0.40 ± 0.02	0.70 ± 0.02

(a) Measuring average rank-correlation (Spearman) between Naive-Bayes scores and SLALOM scores. Linearized performs best.

LM	values v	importances s	lin.	LIME	SHAP
D-BERT	0.68 ± 0.03	0.73 ± 0.02	0.71 ± 0.03	0.67 ± 0.03	0.69 ± 0.03
BERT	0.57 ± 0.04	0.72 ± 0.03	0.64 ± 0.03	0.63 ± 0.03	0.68 ± 0.03
GPT-2	0.67 ± 0.02	0.67 ± 0.02	0.67 ± 0.02	0.64 ± 0.03	0.60 ± 0.03

(b) Measuring average AU-ROC between SLALOM explanations and human token attention. The importance scores are clearly and most strongly predictive of human attention.

LM	values	importances s	lin.	LIME	SHAP	IG	Grad
DistilBERT	0.913 ± 0.053	0.249 ± 0.215	0.915 ± 0.053	0.892 ± 0.068	0.876 ± 0.071	0.360 ± 0.346	0.387 ± 0.344
BERT	0.943 ± 0.048	0.262 ± 0.252	0.944 ± 0.048	0.939 ± 0.056	0.929 ± 0.070	0.093 ± 0.130	0.093 ± 0.129
GPT-2	0.907 ± 0.055	0.294 ± 0.154	0.908 ± 0.055	0.905 ± 0.057	0.895 ± 0.063	0.378 ± 0.203	0.436 ± 0.204

(c) Area Over Perturbation Curve for deletion. Linearized scores performs best in the faithfulness metric.

Table 1: Evaluation of SLALOM scores (“values”, “importance”, “lin.”) with std.errors across explanation quality measures highlights that SLALOM’s different scores serve different purposes.

different signs. Furthermore, we see that some words (“the”) have positive value scores, but a very low importance. This means that they lead to positive scores on their own but are easily overruled by other words. We compare the SLALOM scores obtained on 50 random test samples to a linear Naïve-Bayes model (obtained through counting class-wise word frequencies) as a surrogate ground truth in Table 1a through the Spearman rank correlation. We observe good agreement with the value scores v and the linearized SLALOM scores (“lin”, see Section 5.4).

Evaluating Faithfulness Metrics. Faithfulness metrics quantify the alignment of the explanations with actual model behavior and can be used to compare different explanation techniques. We run the classical removal benchmarks with SLALOM compared to baselines such as LIME [40], SHAP [31], Gradients [48], and Integrated Gradients (IG, [51]). For the deletion benchmark, the tokens with the highest attributions are successively deleted from the sample which should result in a low score for the target class. We iteratively delete more tokens and compute the “Area Over the Perturbation Curve” (AOPC, see [16]), which should be high for deletion. For surrogate techniques (LIME, SHAP, SLALOM) we use 5000 samples each. Our results in Tab. 1c highlight that linearized SLALOM scores outperform LIME and SHAP. Insertion results with similar findings are deferred to Table 8.

Predicting Human Attention. To incorporate a user perspective we predict human attention from SLALOM scores. We compute AU-ROC for predicting annotated human attention as suggested in Sen et al. [45] in Table 1b. We use absolute values of all signed explanations as human attention is unsigned as well. In contrast to the previous experiments, where linearized scores and value scores were more effective, we observe that the importance scores are better at predicting where the human attention is placed, and are more effective than LIME and SHAP. We omit Grad and IG, which perform almost on random level for this task. In summary, these findings highlight the fact that different tasks require different attribution scores and that a single score is insufficient to explain transformer models, as suggested by our theory. SLALOM offers flexibility through its 2-dimensional representation and provides state-of-the-art and efficient attribution explanations on real-world tasks.

7 Discussion and Conclusion

In this work, we established that transformer networks are inherently incapable of aligning with linear or additive models for feature attribution. This may explain similar incapacities observed in time-series forecasting [59], where they

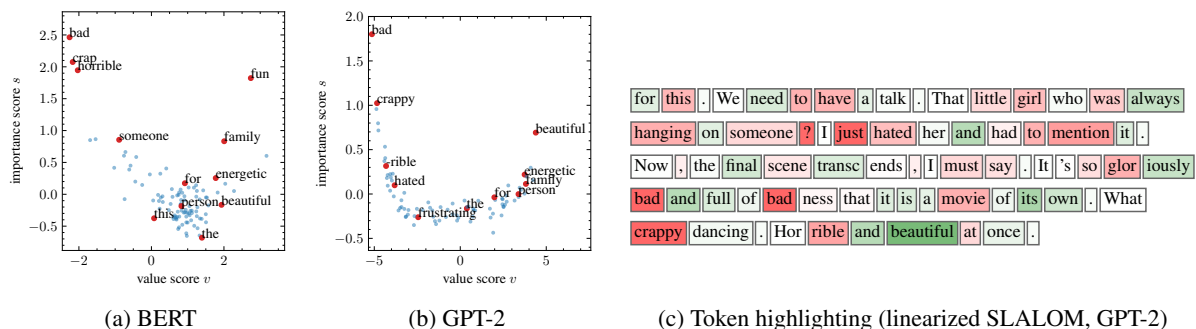


Figure 5: Explaining a real review with SLALOM (qualitative results). SLALOM assigned two scores to each token and can be used to compute attributions. See Figure 11 for fully annotated plots.

seem incapable of representing certain relations. To address this shortcoming, we have introduced the Softmax-Linked Additive Log-Odds Model (SLALOM), a surrogate model for explaining the influence of features on transformers and other complex LMs through a two-dimensional representation. To complement this theoretical foundation, future work will include the evaluation of SLALOM from a user-centric perspective, for instance, on human-centered evaluation frameworks [13]. From a broader perspective, we hope that this research paves the way for advancing the interpretability of widely adopted transformer models.

References

- [1] S. Abnar and W. Zuidema. Quantifying attention flow in transformers. In *Proceedings of the 58th Annual Meeting of the Association for Computational Linguistics*, pages 4190–4197, 2020.
- [2] A. Adadi and M. Berrada. Peeking inside the black-box: a survey on explainable artificial intelligence (xai). *IEEE access*, 2018.
- [3] S. Agarwal, S. Jabbari, C. Agarwal, S. Upadhyay, S. Wu, and H. Lakkaraju. Towards the unification and robustness of perturbation and gradient based explanations. In *International Conference on Machine Learning*, pages 110–119. PMLR, 2021.
- [4] N. Asghar. Yelp dataset challenge: Review rating prediction. *arXiv preprint arXiv:1605.05362*, 2016.
- [5] D. Baehrens, T. Schroeter, S. Harmeling, M. Kawanabe, K. Hansen, and K.-R. Müller. How to explain individual classification decisions. *The Journal of Machine Learning Research*, 11:1803–1831, 2010.
- [6] P. Bartlett, V. Maiorov, and R. Meir. Almost linear vc dimension bounds for piecewise polynomial networks. *Advances in neural information processing systems*, 11, 1998.
- [7] S. Bordt and U. von Luxburg. From shapley values to generalized additive models and back. In *International Conference on Artificial Intelligence and Statistics*, pages 709–745. PMLR, 2023.
- [8] G. Brunner, Y. Liu, D. Pascual, O. Richter, M. Ciaramita, and R. Wattenhofer. On identifiability in transformers. 2020.
- [9] N. Burkart and M. F. Huber. A survey on the explainability of supervised machine learning. *Journal of Artificial Intelligence Research*, 70:245–317, 2021.
- [10] J. Castro, D. Gómez, and J. Tejada. Polynomial calculation of the shapley value based on sampling. *Computers & Operations Research*, 36(5):1726–1730, 2009.
- [11] I. Chalkidis, I. Androutsopoulos, and N. Aletras. Neural legal judgment prediction in english. In *Proceedings of the 57th Annual Meeting of the Association for Computational Linguistics*, pages 4317–4323, 2019.
- [12] H. Chen, G. Zheng, and Y. Ji. Generating hierarchical explanations on text classification via feature interaction detection. *arXiv preprint arXiv:2004.02015*, 2020.
- [13] J. Colin, T. Fel, R. Cadène, and T. Serre. What i cannot predict, i do not understand: A human-centered evaluation framework for explainability methods. *Advances in neural information processing systems*, 35:2832–2845, 2022.
- [14] I. Covert, S. Lundberg, and S.-I. Lee. Explaining by removing: A unified framework for model explanation. *Journal of Machine Learning Research*, 22(209):1–90, 2021.
- [15] J. Devlin, M.-W. Chang, K. Lee, and K. Toutanova. Bert: Pre-training of deep bidirectional transformers for language understanding. *arXiv preprint arXiv:1810.04805*, 2018.
- [16] J. DeYoung, S. Jain, N. F. Rajani, E. Lehman, C. Xiong, R. Socher, and B. C. Wallace. Eraser: A benchmark to evaluate rationalized nlp models. In *Proceedings of the 58th Annual Meeting of the Association for Computational Linguistics*, pages 4443–4458, 2020.
- [17] A. Dolk, H. Davidsen, H. Dalianis, and T. Vakili. Evaluation of lime and shap in explaining automatic icd-10 classifications of swedish gastrointestinal discharge summaries. In *Scandinavian Conference on Health Informatics*, pages 166–173, 2022.
- [18] J. Ferrando and M. R. Costa-jussà. Attention weights in transformer nmt fail aligning words between sequences but largely explain model predictions. *arXiv preprint arXiv:2109.05853*, 2021.
- [19] D. Garreau and U. von Luxburg. Explaining the explainer: A first theoretical analysis of lime. In *International conference on artificial intelligence and statistics*, pages 1287–1296. PMLR, 2020.
- [20] L. H. Gilpin, D. Bau, B. Z. Yuan, A. Bajwa, M. Specter, and L. Kagal. Explaining explanations: An overview of interpretability of machine learning. In *DSAA*, 2018.

- [21] A. Gu and T. Dao. Mamba: Linear-time sequence modeling with selective state spaces. *arXiv preprint arXiv:2312.00752*, 2023.
- [22] T. Han, S. Srinivas, and H. Lakkaraju. Which explanation should i choose? a function approximation perspective to characterizing post hoc explanations. *Advances in Neural Information Processing Systems*, 35:5256–5268, 2022.
- [23] Y. Hao, L. Dong, F. Wei, and K. Xu. Self-attention attribution: Interpreting information interactions inside transformer. In *Proceedings of the AAAI Conference on Artificial Intelligence*, volume 35, pages 12963–12971, 2021.
- [24] Huggingface. Hugging face - models: Most downloaded sequence classification models, 2023. URL https://huggingface.co/models?pipeline_tag=text-classification&sort=downloads.
- [25] S. Jain and B. C. Wallace. Attention is not explanation. *arXiv preprint arXiv:1902.10186*, 2019.
- [26] K. Jeblick, B. Schachtner, J. Dexl, A. Mittermeier, A. T. Stüber, J. Topalis, T. Weber, P. Wesp, B. O. Sabel, J. Rieke, et al. Chatgpt makes medicine easy to swallow: an exploratory case study on simplified radiology reports. *European radiology*, pages 1–9, 2023.
- [27] G. Kasneci and T. Gottron. Licon: A linear weighting scheme for the contribution of input variables in deep artificial neural networks. In *Proceedings of the 25th ACM international on conference on information and knowledge management*, pages 45–54, 2016.
- [28] G. Kobayashi, T. Kuribayashi, S. Yokoi, and K. Inui. Attention is not only a weight: Analyzing transformers with vector norms. In *2020 Conference on Empirical Methods in Natural Language Processing, EMNLP 2020*, pages 7057–7075. Association for Computational Linguistics (ACL), 2020.
- [29] G. Kobayashi, T. Kuribayashi, S. Yokoi, and K. Inui. Feed-forward blocks control contextualization in masked language models. *arXiv preprint arXiv:2302.00456*, 2023.
- [30] T. Le Scao, A. Fan, C. Akiki, E. Pavlick, S. Ilić, D. Hesslow, R. Castagné, A. S. Luccioni, F. Yvon, M. Gallé, et al. Bloom: A 176b-parameter open-access multilingual language model. 2023.
- [31] S. M. Lundberg and S.-I. Lee. A unified approach to interpreting model predictions. *Advances in neural information processing systems*, 30, 2017.
- [32] A. Maas, R. E. Daly, P. T. Pham, D. Huang, A. Y. Ng, and C. Potts. Learning word vectors for sentiment analysis. In *Proceedings of the 49th annual meeting of the association for computational linguistics: Human language technologies*, pages 142–150, 2011.
- [33] S. Maleki, L. Tran-Thanh, G. Hines, T. Rahwan, and A. Rogers. Bounding the estimation error of sampling-based shapley value approximation. *arXiv preprint arXiv:1306.4265*, 2013.
- [34] A. Modarressi, M. Fayyaz, Y. Yaghoobzadeh, and M. T. Pilehvar. Globenc: Quantifying global token attribution by incorporating the whole encoder layer in transformers. In *Proceedings of the 2022 Conference of the North American Chapter of the Association for Computational Linguistics: Human Language Technologies*, pages 258–271, 2022.
- [35] A. Modarressi, M. Fayyaz, E. Aghazadeh, Y. Yaghoobzadeh, and M. T. Pilehvar. DecompX: Explaining transformers decisions by propagating token decomposition. In *Proceedings of the 61st Annual Meeting of the Association for Computational Linguistics (Volume 1: Long Papers)*, pages 2649–2664, 2023.
- [36] C. Molnar. *Interpretable Machine Learning*. 2019.
- [37] Y. Qiang, D. Pan, C. Li, X. Li, R. Jang, and D. Zhu. Attcat: Explaining transformers via attentive class activation tokens. *Advances in Neural Information Processing Systems*, 35:5052–5064, 2022.
- [38] A. Radford, K. Narasimhan, T. Salimans, I. Sutskever, et al. Improving language understanding by generative pre-training. 2018.
- [39] A. Radford, J. Wu, R. Child, D. Luan, D. Amodei, I. Sutskever, et al. Language models are unsupervised multitask learners. *OpenAI blog*, 1(8):9, 2019.
- [40] M. T. Ribeiro, S. Singh, and C. Guestrin. ” why should i trust you?” explaining the predictions of any classifier. In *Proceedings of the 22nd ACM SIGKDD international conference on knowledge discovery and data mining*, pages 1135–1144, 2016.
- [41] Y. Rong, T. Leemann, V. Borisov, G. Kasneci, and E. Kasneci. A consistent and efficient evaluation strategy for attribution methods. In *International Conference on Machine Learning*, pages 18770–18795. PMLR, 2022.

- [42] Y. Rong, T. Leemann, T.-T. Nguyen, L. Fiedler, P. Qian, V. Unhelkar, T. Seidel, G. Kasneci, and E. Kasneci. Towards human-centered explainable ai: A survey of user studies for model explanations. *IEEE Transactions on Pattern Analysis and Machine Intelligence*, 2023.
- [43] V. Sanh, L. Debut, J. Chaumond, and T. Wolf. Distilbert, a distilled version of bert: smaller, faster, cheaper and lighter. *arXiv preprint arXiv:1910.01108*, 2019.
- [44] M. Schirmer, I. M. O. Nolasco, E. Mosca, S. Xu, and J. Pfeffer. Uncovering trauma in genocide tribunals: An nlp approach using the genocide transcript corpus. In *Proceedings of the Nineteenth International Conference on Artificial Intelligence and Law*, pages 257–266, 2023.
- [45] C. Sen, T. Hartvigsen, B. Yin, X. Kong, and E. Rundensteiner. Human attention maps for text classification: Do humans and neural networks focus on the same words? In *Proceedings of the 58th annual meeting of the association for computational linguistics*, pages 4596–4608, 2020.
- [46] S. Serrano and N. A. Smith. Is attention interpretable? In *Proceedings of the 57th Annual Meeting of the Association for Computational Linguistics*, 2019.
- [47] A. Shrikumar, P. Greenside, and A. Kundaje. Learning important features through propagating activation differences. In *International conference on machine learning*, pages 3145–3153. PMLR, 2017.
- [48] K. Simonyan, A. Vedaldi, and A. Zisserman. Deep inside convolutional networks: Visualising image classification models and saliency maps. *arXiv preprint arXiv:1312.6034*, 2013.
- [49] D. Smilkov, N. Thorat, B. Kim, F. Viégas, and M. Wattenberg. Smoothgrad: removing noise by adding noise. *arXiv preprint arXiv:1706.03825*, 2017.
- [50] T. Sun, H. Chen, Y. Qiu, and C. Zhao. Efficient shapley values calculation for transformer explainability. In *Asian Conference on Pattern Recognition*, pages 54–67. Springer, 2023.
- [51] M. Sundararajan, A. Taly, and Q. Yan. Axiomatic attribution for deep networks. In *International conference on machine learning*, pages 3319–3328. PMLR, 2017.
- [52] M. Szczepeński, M. Pawlicki, R. Kozik, and M. Choraś. New explainability method for bert-based model in fake news detection. *Scientific reports*, 11(1):23705, 2021.
- [53] R. Tomsett, D. Harborne, S. Chakraborty, P. Gurram, and A. Preece. Sanity checks for saliency metrics. In *Proceedings of the AAAI Conference on Artificial Intelligence*, volume 34, pages 6021–6029, 2020.
- [54] H. Touvron, L. Martin, K. Stone, P. Albert, A. Almahairi, Y. Babaei, N. Bashlykov, S. Batra, P. Bhargava, S. Bhosale, et al. Llama 2: Open foundation and fine-tuned chat models. *arXiv preprint arXiv:2307.09288*, 2023.
- [55] A. Vaswani, N. Shazeer, N. Parmar, J. Uszkoreit, L. Jones, A. N. Gomez, Ł. Kaiser, and I. Polosukhin. Attention is all you need. *Advances in neural information processing systems*, 30, 2017.
- [56] S. Wiegrefe and Y. Pinter. Attention is not not explanation. *arXiv preprint arXiv:1908.04626*, 2019.
- [57] S. Xu, S. Venugopalan, and M. Sundararajan. Attribution in scale and space. In *Proceedings of the IEEE/CVF Conference on Computer Vision and Pattern Recognition*, pages 9680–9689, 2020.
- [58] S. Yang, S. Huang, W. Zou, J. Zhang, X. Dai, and J. Chen. Local interpretation of transformer based on linear decomposition. In *Proceedings of the 61st Annual Meeting of the Association for Computational Linguistics (Volume 1: Long Papers)*, pages 10270–10287, 2023.
- [59] A. Zeng, M. Chen, L. Zhang, and Q. Xu. Are transformers effective for time series forecasting? In *Proceedings of the AAAI conference on artificial intelligence*, volume 37, pages 11121–11128, 2023.

A Motivation: Failure Cases For Model Recovery

We provide another motivational example that shows a failure case of current explanation methods on transformer architectures. In this example we test the recovery property for a linear model. We create a synthetic dataset where each word in a sequence t has a linear contribution to the log odds score, formalized by

$$\log \frac{p(y = 1|t)}{p(y = 0|t)} = F([t_1, t_2, \dots, t_{|t|}]) = b + \sum_{i=1}^{|t|} w(t_i). \quad (6)$$

We create a dataset of 10 words (cf. Table 2) and train transformer models on samples from this dataset. We subsequently create sequences that repeatedly contain a single token τ (in this case, τ ="perfect"), pass them through the transformers, and use Shapley values (approximated by Kernel-Shap) to explain their output. The result is visualized in Figure 6, and shows that a fully connected model (two-layer, 400 hidden units, ReLU) recovers the correct scores, whereas transformer models fail to reflect the true relationship. This shows that explanation methods that are explicitly or implicitly based on additive models lose their ability to recover the true data-generating process when transformer models are explained.

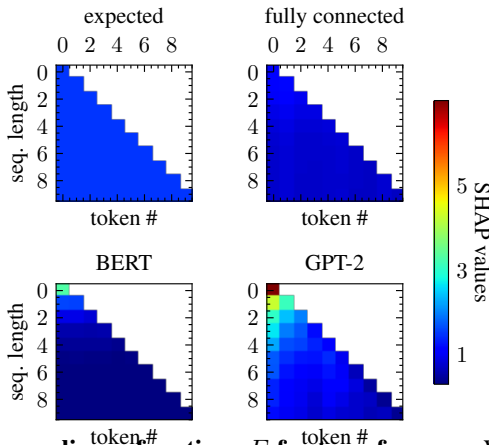


Figure 6: **SHAP values do not recover linear functions F for transformers.** We compute SHAP values for token sequences that repeatedly contain a single token τ with a ground truth score of 1.5 (i.e., $F([\tau])=1.5$, $F([\tau, \tau])=3.0$, ...) such that the ground truth attributions should yield 1.5 independent of the sequence length. While this approximately holds true for a fully connected model, BERT and GPT-2 systematically overestimate the importance for short sequences and underestimate it for longer ones.

B Proofs

B.1 Formalization of the transformer

Many popular LLMs follow the transformer architecture introduced by [55] with only minor modifications. We will introduce the most relevant building blocks of the architecture in this section. A schematic overview of the architecture is visualized in Figure 2. Let us denote the input embeddings for Layer $l \in 1, \dots, L$ by $\mathbf{H}^{(l-1)} = [\mathbf{h}_1^{(l-1)}, \dots, \mathbf{h}_{|t|}^{(l-1)}]^\top \in \mathbb{R}^{|t| \times d}$, where a single line \mathbf{h}_i contains the embedding for token i . The input embeddings of the first layer consist of the token embeddings, i.e., $\mathbf{H}^{(0)} = \mathbf{E}$. At the core of the architecture lies the attention head. For each token, a *query*, *key*, and a *value* vector are computed by applying an affine-linear transform. In matrix notation this can be written as

$$\mathbf{Q}^{(l)} = \mathbf{H}^{(l-1)} \mathbf{W}_Q^{(l)} + \mathbf{1}_{|t|} \mathbf{b}_Q^{(l)\top}, \quad (7)$$

$$\mathbf{K}^{(l)} = \mathbf{H}^{(l-1)} \mathbf{W}_K^{(l)} + \mathbf{1}_{|t|} \mathbf{b}_K^{(l)\top}, \quad (8)$$

$$\mathbf{V}^{(l)} = \mathbf{H}^{(l-1)} \mathbf{W}_V^{(l)} + \mathbf{1}_{|t|} \mathbf{b}_V^{(l)\top}, \quad (9)$$

where $\mathbf{1}_{|t|} \in \mathbb{R}^{|t|}$ denotes a vector of ones of length $|t|$, $\mathbf{b}_Q^{(l)}, \mathbf{b}_V^{(l)}, \mathbf{b}_K^{(l)} \in \mathbb{R}^{d_h}$, $\mathbf{W}_Q^{(l)}, \mathbf{W}_K^{(l)}, \mathbf{W}_V^{(l)} \in \mathbb{R}^{d \times d_h}$, are trainable parameters and d_h denotes the dimension of the attention head.¹ Keys and queries are projected onto each other and

¹We only formalize one attention head here, but consider the analogous case of multiple heads in our formal proofs.

normalized by a row-wise softmax operation,

$$\mathbf{A}^{(l)} = \text{rowsoftmax} \left(\frac{\mathbf{Q}^{(l)} \mathbf{K}^{(l)\top}}{\sqrt{d_k}} \right). \quad (10)$$

This results in the attention matrix $\mathbf{A}^{(l)} \in \mathbb{R}^{|\mathbf{t}| \times |\mathbf{t}|}$, where row i indicates how much the other tokens will contribute to its output embedding. To compute output embeddings, we obtain attention outputs \mathbf{s}_i ,

$$\mathbf{S} = [\mathbf{s}_1, \dots, \mathbf{s}_{|\mathbf{t}|}]^\top = \mathbf{A}^{(l)} \mathbf{V}^{(l)}. \quad (11)$$

Note that an attention output can be computed as $\mathbf{s}_i = \sum_{j=1}^{|\mathbf{t}|} a_{ij} \mathbf{v}_j$, where \mathbf{v}_j denotes the value vector in the line corresponding to token j in $\mathbf{V} = [\mathbf{v}_1, \dots, \mathbf{v}_{|\mathbf{t}|}]^\top$ and $a_{ij} = \mathbf{A}_{i,j}^{(l)}$. The final \mathbf{s}_i are projected back to the original dimension d by some projection operator $P: \mathbb{R}^{d_h} \rightarrow \mathbb{R}^d$ before they are added to the corresponding input embedding $\mathbf{h}_i^{(l-1)}$ due to the skip-connections. The sum is then transformed by a nonlinear function that we denote by $\text{ffn}: \mathbb{R}^d \rightarrow \mathbb{R}^d$. In summary, we obtain the output for the layer, $\mathbf{h}_i^{(l)}$, with

$$\mathbf{h}_i^{(l)} = \text{ffn}_l(\mathbf{h}_i^{(l-1)} + P(\mathbf{s}_i)). \quad (12)$$

This procedure is repeated iteratively for layers $1, \dots, L$ such that we finally arrive at output embeddings $\mathbf{H}^{(L)}$. To perform classification, a classification head $\text{cls}: \mathbb{R}^d \rightarrow \mathbb{R}^{|\mathcal{Y}|}$ is put on top of a token at classification index r (how this token is chosen depends on the architecture, common choices include $r \in \{1, |\mathbf{t}|\}$), such that we get the final logit output $\mathbf{l} = \text{cls}(\mathbf{h}_r^{(L)})$. The logit output is transformed to a probability vector via another softmax operation. Note that in the two-class case, we obtain the log-odds $F(\mathbf{t})$ by taking the difference (Δ) between logits

$$F(\mathbf{t}) := \log \frac{p(y=1|\mathbf{t})}{p(y=0|\mathbf{t})} = \Delta(\mathbf{l}) = \mathbf{l}_1 - \mathbf{l}_0. \quad (13)$$

B.2 Proof of Proposition 4.1

Proposition B.1 (Proposition 4.1 in the main paper). *Let \mathcal{V} be a vocabulary and $C \geq 2, C \in \mathbb{N}$ be a maximum sequence length (context window). Let $w_i: \mathcal{V} \rightarrow \mathbb{R}, \forall i \in 1, \dots, C$ be any mapping that assigns a token encountered at position i a numerical score including at least one token $\tau \in \mathcal{V}$ with non-zero weight $w_i(\tau) \neq 0$ for some $i \in 2, \dots, C$. Let $b \in \mathbb{R}$ be an arbitrary offset. Then, there exists no parametrization of the encoder or decoder single-layer transformer F such that for every sequence $\mathbf{t} = [t_1, t_2, \dots, t_{|\mathbf{t}|}]$ with length $1 \leq |\mathbf{t}| \leq C$, the output of the transformer network is equivalent to*

$$F([t_1, t_2, \dots, t_{|\mathbf{t}|}]) = b + \sum_{i=1}^{|\mathbf{t}|} w_i(t_i). \quad (14)$$

Proof. We show the statement in the theorem by contradiction. Consider the token, $\tau \in \mathcal{V}$, for which $w_j(\tau) \neq 0$ for some token index $j \geq 2$ which exists by the condition in the theorem. We now consider sequences of length k of the form $\mathbf{t}_k = [\underbrace{\tau, \dots, \tau}_{\text{repeat } k \text{ times}}]$ for $k = 1, \dots, C$. For example, we have $\mathbf{t}_1 = [\tau], \mathbf{t}_2 = [\tau, \tau]$, etc. The output of the transformer

is given by

$$F(\mathbf{t}) = g \left(\mathbf{h}_r^{(0)}, \sum_{j=1}^{|\mathbf{t}|} a_{rj} \mathbf{v}_j \right) = g \left(\mathbf{e}(\tau), \sum_{j=1}^{|\mathbf{t}|} \alpha_{rj} \mathbf{v}_j \right), \quad (15)$$

where r is the token index on which the classification head is placed. Note that with $r = |\mathbf{t}|$ for the decoder architecture, the sum always goes up to $|\mathbf{t}|$ (for the encoder architecture this is always true). As all tokens in the sequence have a value of τ , we obtain $\mathbf{h}_r^{(0)} = \mathbf{e}(t_r) = \mathbf{e}(\tau)$. The first input to the final part will thus be equal for all sequences \mathbf{t}_k . We will now show that the second part will also be equal.

We compute the value, key, and query vectors for τ . $\mathbf{v}, \mathbf{k}, \mathbf{q} \in \mathbb{R}^{d_h}$ correspond to one line in the respective key, query and value matrices. As the inputs are identical and we omit positional embeddings in this proof, all lines are identical in the matrices. This results in

$$\mathbf{v} = \mathbf{W}_V^\top \mathbf{e}(\tau) + \mathbf{b}_V \quad (16)$$

$$\mathbf{k} = \mathbf{W}_K^\top \mathbf{e}(\tau) + \mathbf{b}_K \quad (17)$$

$$\mathbf{q} = \mathbf{W}_Q^\top \mathbf{e}(\tau) + \mathbf{b}_Q \quad (18)$$

We omit the layer indices for simplicity. As pre-softmax attention scores (product of key and value vector), we obtain $s = \mathbf{q}^\top \mathbf{k} / \sqrt{d_k}$. Subsequently, the softmax computation will be performed over the entire sequence, resulting in

$$\alpha_r = \text{softmax}(\underbrace{[s, \dots, s]}_{k \text{ times}}) = \left[\frac{\exp(s)}{k \exp(s)} \right] \quad (19)$$

$$= \left[\underbrace{\frac{1}{k}, \dots, \frac{1}{k}}_{k \text{ times}} \right] \quad (20)$$

The second input $\sum_{j=1}^{|\mathbf{t}|} \alpha_{rj} \mathbf{v}_j$ to the feed-forward part is given by

$$\sum_{j=1}^{|\mathbf{t}|} \alpha_{rj} \mathbf{v}_j = \sum_{j=1}^k \alpha_{rj} \mathbf{v}_j = \sum_{j=1}^k \frac{1}{k} \mathbf{v} = \mathbf{v}, \quad (21)$$

as α_{rj} and \mathbf{v} are independent of the token index j . We observe that the total input to final part g is independent of k in its entirety, as the first input $e(\tau)$ is independent of k and the second input is independent of k as well. As g is a deterministic function, also the log-odds output will be the same for all input sequences \mathbf{t}_k and be independent of k . By the condition we have a non-zero weight $w_j(\tau) \neq 0$ for some $j \geq 2$. In this case, there are two sequences \mathbf{t}_{j-1} (length $j-1$) and \mathbf{t}_j (length j) consisting of only token τ , where the outputs of the GAM follow

$$f_{\text{GAM}}(\mathbf{t}_j) = b + \sum_{i=1}^j w_i(\tau) \quad (22)$$

$$= b + \sum_{i=1}^{j-1} w_i(\tau) + w_j(\tau) \quad (23)$$

$$= f_{\text{GAM}}(\mathbf{t}_{j-1}) + w_j(\tau) \quad (24)$$

As we suppose $w_j(\tau) \neq 0$, it must be that $f_{\text{GAM}}(\mathbf{t}_j) \neq f_{\text{GAM}}(\mathbf{t}_{j-1})$ which is a contradiction, with the output being equal for all sequence lengths.

Multi-head attention. In the case of multiple heads, we have

$$F(\mathbf{t}) = \Delta(\text{cls}(\mathbf{h}_r^{(1)})) \quad (25)$$

$$= \Delta(\text{cls}(\text{ffn}(\mathbf{h}_r^{(0)} + \mathbf{P}_{h=1}(\mathbf{s}_r^{h=1}) + \mathbf{P}_{h=2}(\mathbf{s}_r^{h=2}) + \dots + \mathbf{P}_{h=H}(\mathbf{s}_r^{h=H})))) \quad (26)$$

$$= g(\mathbf{h}_r^{(0)}, \mathbf{s}_r^{h=1}, \dots, \mathbf{s}_r^{h=H}) \quad (27)$$

As before, we can make the same argument, if we show that all inputs to g are the same. This is straight-forward, as we can extend the argument made for one head for every head, because none of the head can differentiate between the sequence lengths. The first input will still correspond to $\mathbf{h}_r^{(0)} = e(\tau)$, which results in the same contradiction. \square

B.3 Corollary: Transformers cannot represent linear models

Corollary B.2 (Transformers cannot represent linear models). *Let the context window be $C > 2$ and suppose the same model as in Proposition 4.1. Let $w : \mathcal{V} \rightarrow \mathbb{R}$ be any weighting function that is independent of the token position with $w(\tau) \neq 0$ where for at least one token $\tau \in \mathcal{V}$. Then, the single layer transformer cannot represent the linear model*

$$F([t_1, t_2, \dots, t_N]) = b + \sum_{i=1}^N w(t_i). \quad (28)$$

Proof. This can be seen by setting $w_i \equiv w$ for every i in Proposition 4.1. With $w(\tau) \neq 0$, the condition from Proposition 4.1, i.e., having one w_i with $w_i(\tau) \neq 0$ for $i \geq 2$ is fulfilled as well such that the result of the proposition as well. \square

This statement has a strong implication on the capabilities of transformers as it shows that they struggle to learn linear models.

B.4 Proof of Corollary 4.2

Corollary B.3 (Corollary 4.2 in the main paper). *Under the same conditions as in Proposition 4.1, a stack of multiple transformer blocks as in the model F neither has a parametrization sufficient to represent the linear model.*

Proof. We show the result by induction, with the help of a lemma.

Lemma: Suppose a set S of sequences. If (1) for every sequence $\mathbf{t} \in S$ the input matrix $\mathbf{H}^{(l)} = [\mathbf{h}_1^{(l)}, \dots, \mathbf{h}_{|\mathbf{t}|}^{(l)}]$ will consist of input embeddings that are identical for each token i , and (2) single input embeddings also have the same value for every sequence $\mathbf{t} \in S$, in the output $\mathbf{H}^{(l+1)}$ (1) the output embeddings will be identical for all tokens i and (2) they will have equal value for all the sequences $\mathbf{t} \in S$ considered before.

For the encoder-only architecture, the proof from Proposition 4.1 holds analogously for each token output embedding (in the previous proof, we only considered the output embedding at the classification token r). Without restating the full proof the main steps consist of

- showing the attention to be equally distributed across tokens, i.e., $\alpha_{ij} = 1/|\mathbf{t}|$
- showing the value vectors v_i to be equal because they only depend on the input embeddings which are equal
- concluding that the output will be equal regardless of the number of inputs

This shows that for each sequence $\mathbf{t} \in S$, the output at token i remains constant. To show that all tokens i result in the same output, we observe that the the only dependence of the input token to the output is through the query, which however is also equivalent if we have the same inputs.

For the decoder-only architecture, for token i , the attention weights are taken only up to index i resulting in a weight of $\frac{1}{i}$ for each previous token and a weight of 0 (masked) for subsequent ones. However, with the sum also being equal to 1 and the value vectors being equivalent, there is no difference in the outcome. This proves the lemma.

Having shown this lemma, we consider a set S of two sequences $S = \{\mathbf{t}_{j-1}, \mathbf{t}_j\}$ where \mathbf{t}_{j-1} contains $j-1$ repetitions of token τ and \mathbf{t}_j contains j repetitions of token τ . We chose $j \geq 2, \tau$ such that $w_j(\tau) \neq 0$, which is possible by the conditions of the theorem. We observe that for $\mathbf{H}^{(0)}$, the embeddings are equal for each token and their value is the same for both sequences. We then apply the lemma for layers $1, \dots, L$, resulting in the output embeddings of $\mathbf{H}^{(L)}$ being equal for each token, and most importantly identical for \mathbf{t}_{j-1} and \mathbf{t}_j . As we perform the classification by $F(\mathbf{t}) = \Delta(\text{cls}(\mathbf{h}_r^{(L)}))$, this output will also not change with the sequence length. This result can be used to construct the same contradiction as in the proof of Proposition 4.1. \square

B.5 Proof of Proposition 5.1

Proposition B.4 (Transformers can easily fit SLALOM models). *For any mapping s, v and a transformer with an embedding size $d, d_h \geq 3$, there exists a parameterization of the transformer to reflect the SLALOM model in Equation (4).*

Proof. We can prove the theorem by constructing a weight setup to reflect this mapping. We let the embedding $e(\tau)$ be given by

$$e(\tau) = [s(\tau), v(\tau), 0, 0, \dots, 0]. \quad (29)$$

We then set the key mapping matrix K to be

$$\mathbf{W}_k = \mathbf{0} \quad (30)$$

$$\mathbf{b}_k = [1, 0, \dots, 0]. \quad (31)$$

such that we have

$$\mathbf{W}_k e(\tau) + \mathbf{b}_k = [1, 0, \dots, 0]. \quad (32)$$

For the query mapping we can use

$$\mathbf{W}_q = \mathbf{I} \quad (33)$$

$$\mathbf{b}_q = \mathbf{0} \quad (34)$$

such that

$$\mathbf{W}_v \mathbf{e}(\tau) + \mathbf{b}_v = [s(\tau), v(\tau), 0, \dots, 0]. \quad (35)$$

This results in the non-normalized attention scores for query $\tau \in \mathcal{V}$ and key $\theta \in \mathcal{V}$

$$a(t_i, t_j) = (\mathbf{W}_q \mathbf{e}(t_i) + \mathbf{b}_q)^\top (\mathbf{W}_k \mathbf{e}(t_j) + \mathbf{b}_k) = s(t_j) \quad (36)$$

We see that regardless of the query token, the pre-softmax score will be $s(\theta)$. For the value scores, we perform a similar transform with

$$\mathbf{W}_v = \text{diag}([0, 1, 0, \dots, 0]) \quad (37)$$

$$\mathbf{b}_v = \mathbf{0} \quad (38)$$

such that

$$\mathbf{v}_i = \mathbf{W}_v \mathbf{e}(t_i) + \mathbf{b}_v = [0, 0, v(t_i), 0, \dots, 0]. \quad (39)$$

We then obtain

$$\mathbf{s}_r = \sum_{t_i \in \mathbf{t}} a_{ri} \mathbf{v}_i = \sum_{t_i \in \mathbf{t}} \text{softmax}_i[s(t_1), \dots, s(t_{|\mathbf{t}|})] \mathbf{v}_i \quad (40)$$

$$= \left[0, 0, \sum_{t_i \in \mathbf{t}} \alpha_i(\mathbf{t}) v(t_i), \dots, 0 \right]^\top \quad (41)$$

We saw that the final output can be represented by

$$F(\mathbf{t}) = \Delta(\text{cls}(\text{ffn}(\mathbf{e}(t_0) + P(\mathbf{s}_r)))) \quad (42)$$

The projection operator is linear, which can set to easily forward in input by setting $P \equiv \mathbf{I}$. Due to the skip connection of the feed-forward part, we can easily transfer the second part through the first ffn part. In the classification part, we output the third component and zero by applying the final weight matrix

$$\mathbf{W}_{class} = \begin{bmatrix} 0 & 0 & 0 & \dots & 0 \\ 0 & 0 & 1 & \dots & 0 \end{bmatrix} \quad (43)$$

and a bias vector of $\mathbf{0}$.

Multiple Heads. Multiple heads can represent the pattern by choosing $P = \mathbf{I}$ for one head and choosing $P = \mathbf{0}$ for the other heads.

Multiple Layers. We can extend the argument to multiple layers by showing that the input vectors can just be forwarded by the transformer. This is simple by setting $P \equiv \mathbf{0}$, the null-mapping, which can be represented by a linear operator. We then use the same classification hat as before. \square

B.6 Proof of Proposition 5.2

Proposition B.5 (Proposition 5.2. in the main paper). *Suppose query access to a model G that takes sequences of tokens t with lengths $|\mathbf{t}| \in 1, \dots, C$ and returns the log-odds according to a non-constant SLALOM on a vocabulary \mathcal{V} with unknown parameter mappings $s : \mathcal{V} \rightarrow \mathbb{R}$, $v : \mathcal{V} \rightarrow \mathbb{R}$. For $C \geq 2$, we can recover the true mappings s , v with $2|\mathcal{V}| - 1$ queries (forward passes) of F .*

Proof. We first compute $G([\tau])$, $\forall \tau \in \mathcal{V}$. We know that for single token sequences, all attention is on one token, i.e., ($\alpha_i = 1$) and we thus have

$$G([\tau]) = v(\tau) \quad (44)$$

We have obtained the values scores v for each token through $|\mathcal{V}|$ forward passes. To identify the token importance scores s , we consider token sequences of length 2.

We first note that if the SLALOM is non-constant and $|\mathcal{V}| > 1$, for every token $\tau \in \mathcal{V}$, we can find another token θ for which $v(\tau) \neq v(\theta)$. This can be seen by contradiction: If this would not be the case, i.e., we cannot find a token ω with a different value $v(\omega)$, all tokens have the same value and the SLALOM would have to be constant. For $|\mathcal{V}| = 1$, SLALOM is always constant and does not fall under the conditions of the theorem.

We now select an arbitrary reference token $\theta \in \mathcal{V}$. We select another token $\hat{\theta}$ for which $v(\hat{\theta}) \neq v(\theta)$. By the previous argument such a token always exists if the SLALOM is non-constant. We now compute relative importances w.r.t. θ

that we refer to as η_θ . We let $\eta_\theta(\tau) = s(\tau) - s(\theta)$ denote the difference of the importance between the importance scores of tokens $\tau, \theta \in \mathcal{V}$. We set $\eta_\theta(\theta) = 0$

We start with selecting token $\tau = \hat{\theta}$ and subsequently use each other token $\tau \neq \theta$ to perform the following steps **for each** $\tau \neq \theta$:

1. Identify reference token $\hat{\tau}$. We now have to differentiate two cases: If $v(\tau) = v(\theta)$, we select $\hat{\tau} = \hat{\theta}$ as the reference token. If $v(\tau) \neq v(\theta)$, we select $\hat{\tau} = \theta$ as the reference token. By doing so, we will always have $v(\hat{\tau}) \neq v(\tau)$.

2. Compute $G([\tau, \hat{\tau}])$. We now compute $G([\tau, \hat{\tau}])$. From the model's definition, we know that

$$G([\tau, \hat{\tau}]) = \frac{\exp(s(\tau))}{\exp(s(\tau)) + \exp(s(\hat{\tau}))} v(\tau) \quad (45)$$

$$+ \frac{\exp(s(\hat{\tau}))}{\exp(s(\tau)) + \exp(s(\hat{\tau}))} v(\hat{\tau}) \quad (46)$$

$$= \frac{\exp(s(\tau))}{\exp(s(\tau)) + \exp(s(\hat{\tau}))} G([\tau]) \quad (47)$$

$$+ \frac{\exp(s(\hat{\tau}))}{\exp(s(\tau)) + \exp(s(\hat{\tau}))} G([\hat{\tau}]) \quad (48)$$

$$= \frac{\exp(s(\tau))}{\exp(s(\tau)) + \exp(s(\hat{\tau}))} G([\tau]) \quad (49)$$

$$+ \left(1 - \frac{\exp(s(\tau))}{\exp(s(\tau)) + \exp(s(\hat{\tau}))}\right) G([\hat{\tau}]) \quad (50)$$

which we can rearrange to

$$G([\tau, \hat{\tau}]) - G([\hat{\tau}]) = \frac{\exp(s(\tau))}{\exp(s(\tau)) + \exp(s(\hat{\tau}))} (G([\tau]) - G([\hat{\tau}])) \quad (51)$$

and finally to

$$\frac{\exp(s(\tau))}{\exp(s(\tau)) + \exp(s(\hat{\tau}))} = \frac{G([\tau, \hat{\tau}]) - G([\hat{\tau}])}{G([\tau]) - G([\hat{\tau}])} := g(\tau, \hat{\tau}) \quad (52)$$

and

$$\frac{1}{1 + \frac{\exp(s(\hat{\tau}))}{\exp(s(\tau))}} = g(\tau, \hat{\tau}) \quad (53)$$

$$\Leftrightarrow \frac{1}{g(\tau, \hat{\tau})} = 1 + \frac{\exp(s(\hat{\tau}))}{\exp(s(\tau))} \quad (54)$$

$$\Leftrightarrow \log\left(\frac{1}{g(\tau, \hat{\tau})} - 1\right) = s(\tau) - s(\hat{\tau}) := d(\tau, \hat{\tau}) \quad (55)$$

This allows us to express the importance of every token $\tau \in \mathcal{V}$ relative to the base token $\hat{\tau}$.

3. Compute importance relative to θ , i.e., $\eta_\theta(\tau)$. In case we selected $\hat{\tau} = \theta$, we set $\eta_\theta(\tau) = d(\tau, \hat{\tau}) = s(\tau) - s(\theta)$.

In case we selected $\hat{\tau} = \hat{\theta}$, we set

$$\eta_\theta(\tau) = d(\tau, \hat{\tau}) - d(\hat{\theta}, \theta) = s(\tau) - s(\hat{\theta}) + (s(\hat{\theta}) - s(\theta)) = s(\tau) - s(\theta) \quad (56)$$

The value of $d(\hat{\theta}, \theta)$ is already known from the first iteration of the loop, where we consider $\tau = \hat{\theta}$ (and needs to be computed only once).

Having obtained a value of $\eta_\theta(\tau)$ for each token $\tau \neq \theta$, with $|\mathcal{V}| - 1$ forward passes, we can then use the normalization in constraint to solve for $s(\theta)$ as in

$$\sum_{\tau \in \mathcal{V}} (\eta_\theta(\tau) + s(\theta)) = |\mathcal{V}| \cdot 0 \quad (57)$$

such that we obtain

$$s(\theta) = \frac{\sum_{\tau \in \mathcal{V}} \eta_\theta(\tau)}{|\mathcal{V}|} \quad (58)$$

We can plug this back in to obtain the values for all token importance scores $s(\tau) = s(\theta) + \eta_\theta(\tau)$. We have thus computed the mappings s and v in $2|\mathcal{V}| - 1$ forward passes, which completes the proof. \square

B.7 Relating SLALOM to other attribution techniques.

Local Linear Attribution Scores. We can consider the following weighted model:

$$F(\boldsymbol{\lambda}) = \frac{\sum_{t_i \in \mathbf{t}} \lambda_i \exp(s(t_i)) v(t_i)}{\sum_{t_i \in \mathbf{t}} \lambda_i \exp(s(t_i))} \quad (59)$$

where $\lambda_i = 1$ if a token is present and $\lambda_i = 0$ if it is absent. We observe that setting $\lambda_i = 0$ has the desired effect of making the output of the weighted model equivalent to that of the unweighted SLALOM on a sequence without this token.

Taking the derivative at $\boldsymbol{\lambda} = \mathbf{1}$ results in

$$\frac{\partial F}{\partial \lambda_i} = \frac{\exp(s(t_i)) v(t_i) (\sum_{t_j \in \mathbf{t}, j \neq i} \lambda_j \exp(s(t_j)))}{(\sum_{t_j \in \mathbf{t}} \lambda_j \exp(s(t_j)))^2} \quad (60)$$

$$- \frac{\exp(s(t_i)) (\sum_{t_j \in \mathbf{t}, j \neq i} \lambda_j \exp(s(t_j)) v(t_j))}{(\sum_{t_j \in \mathbf{t}} \lambda_j \exp(s(t_j)))^2} \quad (61)$$

Plugging in $\boldsymbol{\lambda} = \mathbf{1}$, and using $\alpha_i(\mathbf{t}) = \frac{\exp(s(t_i))}{\sum_{t_j \in \mathbf{t}} \lambda_j \exp(s(t_j))}$ we obtain

$$\left. \frac{\partial F}{\partial \lambda_i} \right|_{\boldsymbol{\lambda}=\mathbf{1}} = \alpha_i (v(t_i)(1 - \alpha_i(\mathbf{t})) - (F(\mathbf{1}) - \alpha_i v(t_i))) \quad (62)$$

$$= \alpha_i ((v(t_i) - \alpha_i v(t_i))) - (F(\mathbf{1}) - \alpha_i v(t_i)) \quad (63)$$

$$= \alpha_i (v(t_i) - F(\mathbf{1})) \quad (64)$$

Noting that $\alpha_i = \frac{\exp(s(t_i))}{R}$, where R and $F(\mathbf{1})$ are independent of i , we obtain

$$\left. \frac{\partial F}{\partial \lambda_i} \right|_{\boldsymbol{\lambda}=\mathbf{1}} \propto v(t_i) \exp(s(t_i)), \quad (65)$$

which can be used to rank tokens according the locally linear attributions. We refer to this expression as linearized SLALOM scores (“lin”).

Shapley Values. We can convert SLALOM scores to Shapley values $\phi(i)$ using the explicit formula:

$$\phi(i) = \frac{1}{n} \sum_{S \in [N] \setminus \{i\}} \binom{n-1}{|S|} (F(S \cup \{i\}) - F(S)) \quad (66)$$

$$= \frac{1}{n} \sum_{S \in [N] \setminus \{i\}} \binom{n-1}{|S|} \left(F(S \cup \{i\}) - \frac{F(S \cup \{i\}) - \alpha_i v_i}{1 - \alpha_i} \right) \quad (67)$$

$$= \frac{1}{n} \sum_{S \in [N] \setminus \{i\}} \binom{n-1}{|S|} \left(\frac{\alpha_i (v_i - F(S \cup \{i\}))}{1 - \alpha_i} \right) \quad (68)$$

$$\left(\frac{\alpha_i (v_i - F(\mathbf{1}))}{1 - \alpha_i} \right) \quad (69)$$

However, computing this sum remains usually intractable, as the number of coalitions grows exponentially. We can resort to common sampling approaches [10, 33] to approximate the sum.

C Additional Discussion and Intuition

C.1 Generalization to multi-class problems

We can imagine the following generalizing SLALOM to multi class problems as follows: Suppose we have an importance mapping $s : \mathcal{V} \rightarrow \mathbb{R}$ that still maps each token to an importance score. However, we now introduce a value score mapping $v_c : \mathcal{V} \rightarrow \mathbb{R}$ for each class $c \in \mathcal{Y}$. Additionally to requiring

$$\sum_{\tau \in \mathcal{V}} s(\tau) = 0. \quad (70)$$

we now require

$$\sum_{c \in \mathcal{Y}} v_c(\tau) = 0, \forall \tau \in \mathcal{V} \quad (71)$$

For an input sequence \mathbf{t} , the SLALOM model then computes

$$F_c(\mathbf{t}) = \log \frac{p(y = 1|\mathbf{t})}{p(y = 0|\mathbf{t})} = \sum_{\tau_i \in \mathbf{t}} \alpha_i(\mathbf{t}) v_c(t_i), \quad (72)$$

The posterior probabilities can be computed by performing a softmax operation over the F -scores, as in

$$p(y = c|\mathbf{t}) = \frac{\exp(F_c(\mathbf{t}))}{\sum_{c' \in \mathcal{Y}} \exp(F_{c'}(\mathbf{t}))} \quad (73)$$

We observe that this model has $(|\mathcal{Y}| - 1)|\mathcal{V}| - 1$ free parameters (for the two-class problem, this yields $2|\mathcal{V}| - 1$ as before) and can be fitted and deployed as the two-class SLALOM without major ramifications.

D Algorithm: Local SLALOM approximation

We propose the following algorithm to explain a sequence $\mathbf{t} = [t_1, \dots, t_{|\mathbf{t}|}]$ with SLALOM scores. In particular, we use the Mean-Squared-Error (MSE) to fit SLALOM on random sequences consisting of the individual tokens in the sequence. The procedure is given in Algorithm 1. To speed up the fitting we can sample a large collection of samples before the fitting loop and only sample minibatches from this collection in each step. We perform this optimization and use $b = 5000$ samples in this work. We use sequences of length $n = 2$.

Algorithm 1 Local SLALOM approximation

Require: Sequence \mathbf{t} , trained model F (outputs log odds), random sample length n , learning rate λ , batch size r , sample pool size b , number of steps c

Initialize $v(t_i) = 0, s(t_i) = 0 \quad \forall$ unique $t_i \in \mathbf{t}$

$B \leftarrow b$ samples of random sequences of length n obtained through uniform sampling of unique tokens in \mathbf{t} .

Precompute $F(B[i]), i = 1, \dots, b$ # perform model forward-pass for each sample in pool

steps $\leftarrow 0$

while steps $< c$ **do**

$B' \leftarrow$ minibatch of r samples uniformly sampled from the sample pool B

loss $\leftarrow \frac{1}{r} \sum_{k=1}^r (F(B'[k]) - \text{SLALOM}_{v,s}(B'[k]))^2$ # compute MSE btw. F and SLALOM using precomputed models outputs $F(B')$

$v \leftarrow v - \lambda \nabla_v \text{loss}$ # Back-propagate loss to update SLALOM parameters

$s \leftarrow s - \lambda \nabla_s \text{loss}$

steps \leftarrow steps + 1

end while

return $v, s - \text{mean}(s)$ # normalize s to zero-mean

E Experimental Details

In this section, we provide details on the experimental setups. We provide the full source-code for the experimental evaluation in a ZIP file along with this submission to enhance reproducibility. We fully commit to open-sourcing our code in case of acceptance.

E.1 Fitting transformers on a synthetic dataset

E.1.1 Dataset construction

We create a synthetic dataset to ensure a linear relationship between features and log-odds. Before sampling the dataset, we fix a vocabulary of tokens, ground truth scores for each token, and their occurrence probability. This means that each of the possible tokens already comes with a ground-truth score w that has been manually assigned. The tokens, their respective scores w , and occurrence probabilities are listed in Table 2. Samples of the dataset are sampled in four steps that are executed repeatedly for each sample:

word	“the”	“we”	“movie”	“watch”	“good”	“best”	“perfect”	“ok”	“bad”	“worst”
linear weight w	0.0	0.0	0.0	0.0	0.6	1.0	1.5	-0.6	-1.0	-1.5
$p_{\text{occurrence}}$	1/6	1/6	1/6	1/6	1/15	1/20	1/20	1/15	1/20	1/20

Table 2: Tokens in the linear dataset with their corresponding weight

1. A sequence length $|t| \sim \text{Bin}(p = 0.5, n=30)$ is binomially distributed with an expected value of 15 tokens and a maximum of 30 tokens
2. We sample $|t|$ tokens independently from the vocabulary according to their occurrence probability (Table 2)
3. Third, having obtained the input sequence, we can evaluate the linear model by summing up the scores of the individual tokens in a sequence:

$$F(\mathbf{t}) = F([t_1, t_2, \dots, t_{|t|}]) = \sum_{i=1}^{|t|} w(t_i). \quad (74)$$

4. Having obtained the log-odds ratio for this sample $F(\mathbf{t})$, we sample the labels according to this ratio. We have $p(y = 1)/p(y = 0) = \exp(F(\mathbf{t}))$, which can be rearranged to $p(y = 1) = \frac{\exp(F(\mathbf{t}))}{1 + \exp(F(\mathbf{t}))}$. We sample a binary label y for each sample according to this probability.

The tokens appear independently with the probability $p_{\text{occurrence}}$ given in the table.

E.1.2 Post-hoc fitting of surrogate models

We train the models on this dataset for 5 epochs, where one epoch contains 5000 samples at batch size of 20 using default parameters otherwise.

For the results in Figure 3, we query the models with sequences that contain growing numbers of the work perfect, i.e. [“perfect”, “perfect”, ...]. We prepend a CLS token for the BERT models.

For the results in Figure 4, we then sample 10000 new samples from this dataset and forward them through the trained transformers. The model log-odds score together with the feature vectors are used to train the different surrogate models, linear model, GAM, and SLALOM. For the linear model, we fit an OLS on the log-odds returned by the model. We use the word counts for each of the 10 tokens as a feature vector. The GAM provides the possibility to assign each token a different weight according to its position in the sequence. To this end, we use a different feature vector of length $30 \cdot 10$. Each feature corresponds to a token and a position and is set to one if the token i is present at this position, and set to 0 otherwise. We then fit a linear model using regularized (LASSO) least squares with a small regularization constant of $\lambda = 0.01$.

E.2 Recovering SLALOMs from observations

We resort to a second synthetic dataset to study the recovery property for the SLALOM. To find a realistic distribution of scores, we compute a BoW importance scores for input tokens of the BERT model on the IMDB dataset by counting the class-wise occurrence probabilities. We select 200 tokens randomly from this dataset. We use these scores as value scores v but multiply them by a factors of 2 as many words have very small BoW importances. In realistic datasets, we observed that value scores v are correlated with the importance scores s . Therefore, we sample

$$s(\tau) \sim 5 \left(v(\tau)^{\frac{3}{2}} \right) + \frac{1}{2} \mathcal{N}(0, 1), \quad (75)$$

which results in the value/importance distribution given in Figure 7. We assign each word an equal occurrence probability and sample sequences of words at uniformly distributed lengths in random $[1, 30]$. After a sequence is sampled, labels are subsequently sampled according to the log-odds ratio of the SLALOM. We train the transformer models on $20 \cdot 20000$ samples. When using a smaller vocabulary size, we only sample the sequences out of the first $|\mathcal{V}|$ possible tokens.

E.3 Training Details for Real-World data experiments

Training details. In these experiments, we use the IMDB [32] and Yelp [4] datasets to train transformer models on. Specifically, the results in Table 1a are obtained by training 2-layer versions of BERT, DistilBERT and GPT-2 with on 5000 samples from the IMDB dataset for 1 epoch, respectively. We did not observe significant variation in terms

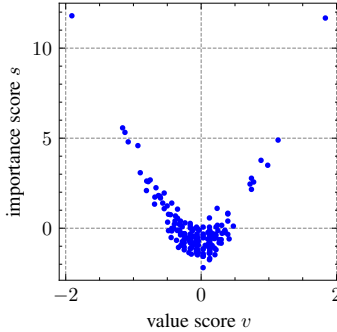


Figure 7: Score distribution for the tokens for the analytical SLALOM used in the recovery experiment.

dataset	DistilBERT	BERT	GPT-2
IMDB	0.84	0.74	0.81
Yelp	0.91	0.89	0.91

Table 3: **Accuracies of models used in this paper.** For IMDB ($|trainset| = 5000$), we use 2-layer versions of the models. For Yelp, ($|trainset| = 25000$), we use 1-layer versions of the models. For both datasets, the $|testset| = 5000$. The models are trained for 1 epoch after which we found the accuracy of the model on the test set to be converged.

of number of layers, so we stick to the simpler models for the final experiments. For the experiments in Table 1b we train 1-layer versions of the above models for 1 epoch on 25000 samples of the Yelp dataset. We report the accuracies of these models in Table 3 and additional hyperparameters in Table 4.

SLALOM vs. Naïve Bayes Ground Truth. To arrive at the Spearman rank-correlations between SLALOM importance scores s , value scores v and their combination ($\exp(s) \cdot v$) with a ground truth, we fit SLALOM on each of the trained models and use a Naïve-Bayes model for ground truth scores. The model is given as follows:

$$\log \frac{p(y = 1|\mathbf{t})}{p(y = 0|\mathbf{t})} = \log \frac{p(y = 1)}{p(y = 0)} + \sum_{t_i \in \mathbf{t}} \log \frac{p(t_i|y = 1)}{p(t_i|y = 0)} \quad (76)$$

We obtain $\frac{p(t_i|y=1)}{p(t_i|y=0)}$ by counting class-wise word frequencies, such that we obtain a linear score w for each token τ given by $w(\tau) = \frac{(\#\text{occ. of } \tau \text{ in class 1}) + \alpha}{(\#\text{occ. of } \tau \text{ in class 0}) + \alpha}$. We use Laplace smoothing with $\alpha = 40$. The final correlations are computed over a set of 50 random samples, where we observe good agreement between the Naïve Bayes scores, and the value and linearized SLALOM scores, respectively. Note that the importance scores are considered unsigned, such that we compute their correlation with the absolute value of the Naive Bayes scores.

SLALOM vs. Human Attention. The Yelp Human Attention (HAT) [45] dataset consists of samples from the original Yelp review dataset, where for each review real human annotators have been asked to select the words they deem important for the underlying class (i.e. positive or negative). This results in binary attention vectors, where each word either is or is not important according to the annotators. Since each sample is processed by multiple annotators, we use the consensus attention map as defined in Sen et al. [45] to aggregate them into one attention vector per sample. Since HAT, unlike SLALOM, operates on a word level, we map each word’s human attention to each of its tokens (according to the employed model’s specific tokenizer).

To compare SLALOM scores with human attention in Table 1b, we choose the AU-ROC metric, where the binary human attention serves as the correct class, and the SLALOM scores as the prediction. We observe how especially the importance scores of SLALOM are reasonably powerful in predicting human attention. Note that the human attention scores are unsigned, such that we also use absolute values for the SLALOM value scores and the linearized version of the SLALOM scores for the HAT prediction.

F Additional Experimental Results

F.1 Fitting SLALOM as a Surrogate to Transformer outputs

We report Mean-Squared Errors when fitting SLALOM to transformer models trained on the linear dataset in Table 5. These results underline that SLALOM outperforms linear and additive models when fitting them to the transformer

parameter	value	specification	value
learning rate	5e-5	CPU core:	AMD EPYC 7763
batch size	5	Num. CPU cores	64-Core (128 threads)
epochs	1	GPU type used	1xNvidia A100
dataset size	5000	GPU-RAM	80GB
number of heads	6	Compute-Hours	≈ 150 h
num. parameter	31M - 124M		

(a) Hyperparameters

(b) Hardware used (internal cluster)

Table 4: Overview over relevant hyperparameters and hardware

architecture	L (num.layers)	linear model	GAM	SLALOM
GPT-2	1	20.31 ± 2.02	48.78 ± 2.70	16.92 ± 1.33
GPT-2	2	24.81 ± 3.11	54.33 ± 3.26	22.17 ± 1.98
GPT-2	6	32.66 ± 7.60	57.08 ± 7.19	21.59 ± 4.14
GPT-2	12	25.74 ± 4.18	54.36 ± 3.94	20.25 ± 2.37
DistilBERT	1	28.28 ± 4.30	44.43 ± 2.22	10.83 ± 2.13
DistilBERT	2	32.58 ± 7.75	53.87 ± 7.20	16.82 ± 4.38
DistilBERT	6	31.49 ± 4.06	49.35 ± 3.13	17.26 ± 3.64
DistilBERT	12	50.82 ± 9.21	71.64 ± 9.19	27.50 ± 4.18
BERT	1	26.33 ± 1.90	43.30 ± 0.88	7.34 ± 0.70
BERT	2	28.43 ± 3.75	48.28 ± 3.23	9.92 ± 1.19
BERT	6	50.82 ± 6.34	68.23 ± 4.59	23.99 ± 3.38
BERT	12	44.58 ± 13.15	51.38 ± 14.71	18.77 ± 6.78

Table 5: MSE ($\times 100$) when fitting SLALOM to the outputs of transformer models trained on the linear dataset. SLALOM manages to describe the outputs of the transformer significantly better than other surrogate models *even if the underlying relation in the data was linear*.

outputs. Note that even if the original relation in the data was linear, the transformer does not represent this relation such that the SLALOM describes its output better. We present additional qualitative results for other models in Figure 8 that support the same conclusion.

F.2 Fitting SLALOM on Transformers trained on data following the SLALOM distribution

We report Mean-Squared Errors in the logit-space and the parameter-space between original SLALOM scores and recovered scores. The logit output are evaluated on a test set of 200 samples that are sampled from the original SLALOM. We provide these quantitative results in Table 6 for logit scores the result are very small Table 7. In logits the differences are negligibly small, and seem to decrease further with more layers. This finding highlight that a) transformers with more layers still easily fit SLALOMs and such model can be recovered in parameters space. The results on the MSE in parameter space show no clear trend, but are relatively small as well (with the largest value being MSE=0.015 (note that results in the table are multiplied by a factor of 100 for readability). Together with our quantitative results in Figure 4, this highlight that SLALOM has effective recovery properties.

L (num.layers)	DistilBERT	BERT	GPT-2
1	0.002 ± 0.001	0.002 ± 0.000	0.011 ± 0.009
2	0.003 ± 0.002	0.003 ± 0.002	0.017 ± 0.011
6	0.001 ± 0.001	0.011 ± 0.007	<0.001 ± 0.000
12	<0.001 ± 0.000	<0.001 ± 0.000	<0.001 ± 0.000

Table 6: MSE ($\times 100$), logit space, averaged over 5 runs

L (num.layers)	DistilBERT	BERT	GPT-2
1	0.092 ± 0.045	0.540 ± 0.301	0.940 ± 0.392
2	0.094 ± 0.049	0.368 ± 0.085	1.652 ± 0.903
6	0.124 ± 0.030	0.830 ± 0.182	0.569 ± 0.177
12	0.287 ± 0.088	0.394 ± 0.255	0.385 ± 0.126

Table 7: MSE ($\times 100$), parameter space, averaged over 5 runs

F.3 Comparing SLALOM-SGD and SLALOM-Ana

We test our two fitting algorithms for different context lengths and vocabulary sizes. We report averages over 15 runs and present the results in Figure 9. We find that in the parameter space, SLALOM-Ana and SLALOM-SGD yield similar approximation quality. On the logit outputs, the SGD method results in a lower, almost constant approximation error whereas this error increases drastically for high context lengths when using SLALOM-Ana. This is not unexpected, as the analytical solution only uses short sequences to estimate the model. We therefore resort to SLALOM-SGD in our final study.

F.4 Real-World Data

We obtain SLALOM explanations for real-world data using the procedure outlines in Algorithm 1 with sequences of length $n = 3$.

In Figure 10 we show a sample from the Yelp HAT dataset. To visualize the attention of SLALOM, we train a 1-layer BERT model with 12 attention heads for 1 epoch on reviews from the Yelp dataset. After fitting SLALOM on top of the resulting model, we can extract the importance scores given to each token in the sample. We can see that the SLALOM scores manage to identify many of the tokens which real human annotators also deemed important for this review to be classified as positive.

Figure 11 shows the full results from the sample used in Figure 5, where we only visualized a choice of words for readability purposes. For this, we train 2-layer, 12-head BERT and GPT-2 models on the IMDB dataset for 1 epoch, respectively. After fitting SLALOM on these models, we use it to explain a movie review taken from the dataset, visualizing value scores v against importance scores s .

F.5 Removal Benchmarks

It is important to verify that SLALOM scores are competitive to other methods in classical explanation benchmarks as well. We therefore ran the classical removal and insertion benchmarks with SLALOM compared to baselines such as LIME, SHAP, Grad [48], and Integrated Gradients (IG, [51]). For the insertion benchmarks, the tokens with the highest attributions are inserted to quickly obtain a high prediction score to the target class. For the deletion benchmark, the tokens with the highest attributions are deleted from the sample to obtain a low score for the target class. We subsequently delete/insert more tokens and compute the ‘‘Area Over the Perturbation Curve’’ (AOPC) as in DeYoung et al. [16], which should be high for deletion and low for insertion. In addition to the deletion results in Table 1c, the insertion results are shown in Table 8. Our linear SLALOM scores perform par with LIME and SHAP in this benchmark. For surrogate techniques (LIME, SHAP, SLALOM) we use 5000 samples each. As a model, we use a 6-layer models for each of the named architectures.

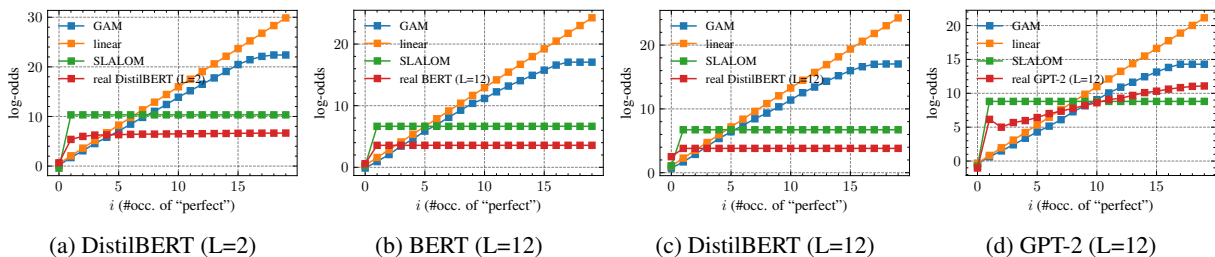
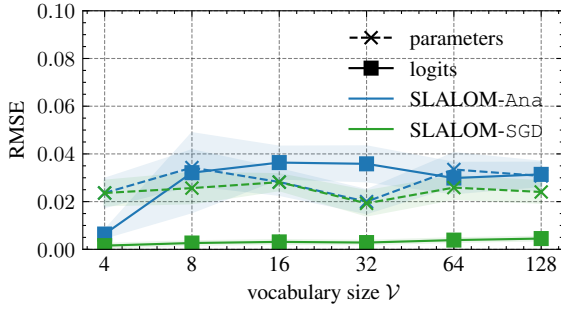
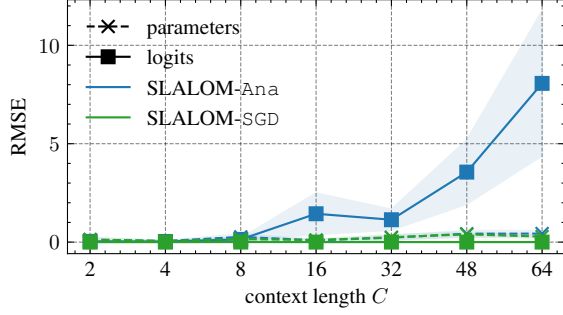


Figure 8: **SLALOM describes outputs of transformer models well.** Fitting SLALOM to the outputs of the models shown in Figure 3. Results on additional models. Despite having $C/2=15\times$ more parameters than the SLALOM model, the GAM model does not describe the output as accurately. We provide quantitative results in Table 5.



(a) Effect of vocabulary size $|\mathcal{V}|$



(b) SLALOM-Ana vs. SLALOM-SGD for different C

Figure 9: SLALOM-Ana vs. SLALOM-SGD for different context lengths C and vocabulary sizes $|\mathcal{V}|$

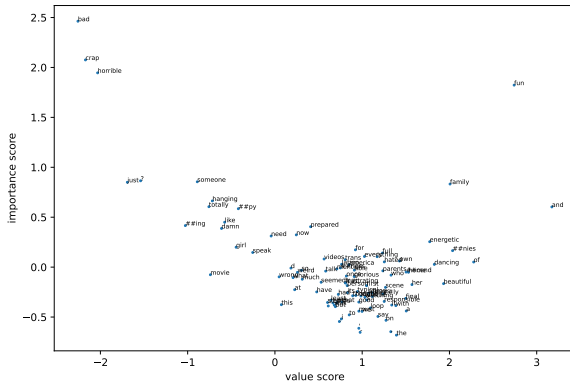
the most delicious steak [] [] we ever had [] also the most expensive [] but it was totally worth it [] our waiter was incredible [] as was his assistant [] and we loved the vibe of the restaurant [] not too stuffy [] really fun [] great cocktail s [] if [] [] m ever back in vegas [] [] [] d love to return []

(a) SLALOM importance scores

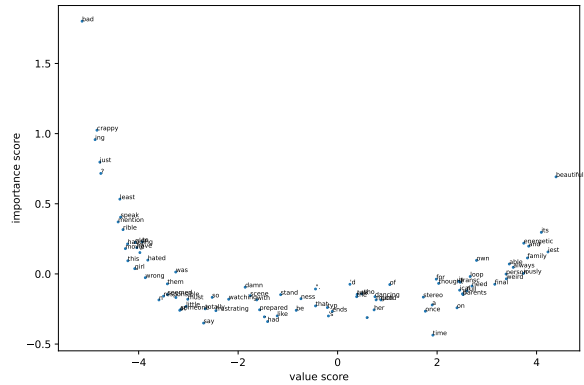
the most delicious steak [] [] we ever had [] also the most expensive [] but it was totally worth it [] our waiter was incredible [] as was his assistant [] and we loved the vibe of the restaurant [] not too stuffy [] really fun [] great cocktail s [] if [] [] m ever back in vegas [] [] [] d love to return []

(b) Human Attention

Figure 10: **SLALOM importance scores compared to human attention.** Fitting SLALOM to the outputs of a 1-layer BERT model trained on Yelp reviews. Many words deemed important by human annotators are likewise highlighted by SLALOM.



(a) BERT



(b) GPT-2

Figure 11: Full scatter plots of SLALOM scores for the sample shown in the main paper (please zoom in for details). We observe that words like “bad” or “fun” get assigned high importance scores and value scores of high magnitude (albeit with different signs) by SLALOM.

LM	values v	importances s	lin. SLALOM	LIME	SHAP	IG	Grad
GPT-2	0.088 ± 0.061	0.531 ± 0.209	0.088 ± 0.061	0.089 ± 0.062	0.100 ± 0.071	0.617 ± 0.191	0.559 ± 0.191
BERT	0.011 ± 0.005	0.293 ± 0.199	0.010 ± 0.004	0.009 ± 0.004	0.010 ± 0.006	0.482 ± 0.275	0.497 ± 0.280
DistilBERT	0.041 ± 0.020	0.442 ± 0.336	0.040 ± 0.019	0.041 ± 0.021	0.044 ± 0.025	0.439 ± 0.335	0.343 ± 0.319

Table 8: Area-Over Perturbation Curve (insertion, lower is better)

	SHAP	LIME	lin. SLALOM
Insertion (lower)	0.0120 \pm 0.005	0.0053 \pm 0.003	0.0039 \pm 0.001
Deletion (higher)	0.8022 \pm 0.026	0.9481 \pm 0.005	0.9601 \pm 0.004

Table 9: AOPC explanation fidelity metrics for the Fully Connected TF-IDF model. The scores highlight that SLALOM can also provide faithful explanations for non-transformer models due to its general expressivity.

(a) BERT

Runtime (s)	SHAP	LIME	IG	Grad	SLALOM
1000 Samples	3.89 \pm 0.21	1.55 \pm 0.22	0.05 \pm 0.01	0.01 \pm 0.01	0.24 \pm 0.02
3000 Samples	13.70 \pm 0.29	4.69 \pm 0.66	0.05 \pm 0.01	0.01 \pm 0.01	0.71 \pm 0.01
10000 Samples	45.54 \pm 0.80	15.57 \pm 2.20	0.05 \pm 0.01	0.01 \pm 0.01	2.40 \pm 0.02

(b) BLOOM-7B

Runtime (s)	SHAP	LIME	IG	Grad	SLALOM
1000 Samples	25.04 \pm 2.37	15.73 \pm 2.37	0.29 \pm 0.04	0.06 \pm 0.01	0.62 \pm 0.02

Table 10: Runtime results for computing different explanations. SLALOM is substantially more efficient than other surrogate model explanations (e.g., LIME, SHAP). Gradient-based explanations can be computed even quicker, but are very noisy and require backward passes. Runtimes are given in seconds (s).

F.6 Error Analysis for non-transformer models

We also investigate the behavior of SLALOM for models that do not precisely follow the architecture described in the Analysis section of this paper. In the present work, we consider an attribution method that is specifically catered towards the transformer architecture, which is the most prevalent in sequence classification. Indeed, we observe mid-sized transformer models like BERT to be prevalent in sequence classification. On the huggingface hub, among the 10 most downloaded models, 9 are BERT-based and the remaining one is another transformer with around 33M parameters (MiniLM). We advise caution when using our model when the type of underlying LM is unknown. In this case, model-agnostic interpretability methods may be preferred. However, we investigate this issue further: We applied our SLALOM approach to a simple, non-transformer sequence classification model on the IMDB dataset, which is a three-layer feed-forward network based on a TF-IDF representation of the inputs. We compute the insertion and deletion Area-over-perturbation-curve metrics that are given in Table 9.

These results show that due to its general expressivity, the SLALOM model also succeeds to provide explanations for non-transformer models that outperform LIME and SHAP in the removal and insertion tests. We also invite the reader to confer Table 12 and Appendix F.8, where we show that SLALOM can predict human attention for large models, including the non-transformer Mamba model [21].

F.7 Runtime analysis

We ran SLALOM as well as other feature attribution methods using surrogate models and compared their runtime to explain a single classification of a 6-layer BERT model. We note that the runtime is mainly determined by the number of forward passes to obtain the samples to fit the surrogates. While this number is independent of the dataset size, longer sequences require more samples for the same approximation quality. The results are shown in Table 10.

While IG and Gradient explanations are the quickest, they also require backward passes which have large memory requirements. As expected, the computational complexity for surrogate model explanation (LIME, SHAP, SLALOM) is dominated by the number of samples and forward passes done. **Our implementation of SLALOM is around 8-10x faster than LIME and almost 20x faster than SHAP** (all approaches used a GPU-based, batching-enabled implementation), which we attribute to the fact that SLALOM can be fitted using substantially shorter sequences than are used by LIME and SHAP.

We are interested to find out how many samples are required to obtain an explanation of comparable quality to SHAP. We successively increase the number of samples used to fit our surrogates and report the performance in the deletion benchmark (where the prediction should drop quickly when removing the most im-

Number of samples	Deletion AOPC
SHAP (nsamples="auto")	0.9135 \pm 0.0105
SLALOM, 500 samples	0.9243 \pm 0.0105
SLALOM, 1000 samples	0.9236 \pm 0.005
SLALOM 2000 samples	0.9348 \pm 0.005
SLALOM, 5000 samples	0.9387 \pm 0.005
SLALOM, 10000 samples	0.9387 \pm 0.005

Table 11: Ablation study on the number of samples required to obtain good explanations. The results highlight that a number as low as 500 samples can be sufficient to fit the surrogate model at a quality comparable to SHAP.

LM	values v	importances s	lin. ($\exp(s) \cdot v$)
BLOOM-7B	0.69 \pm 0.01	0.71 \pm 0.02	0.70 \pm 0.02
Mamba-2.8B	0.69 \pm 0.02	0.32 \pm 0.02	0.70 \pm 0.01

Table 12: ROC-Scores for predicting Human attention with SLALOM using LLMs

portant tokens). We report the Area over the Perturbation Curve (AOPC) as before (this corresponds to their Comprehensiveness metric of ERASER[16], higher scores are better). We compare the performance to `shap.KernelExplainer.shap_values(nsamples=auto)` method of the shap package in Table 11. Our results indicate that sampling sizes as low as 500 per explained instance (which is as low as predicted by our theory, with average sequence length of 200) already yields competitive results.

F.8 Applying SLALOM to Large Language Models

Our work is mainly concerned with sequence classification. In this application, we observe mid-sized models like BERT to be prevalent. On the huggingface hub, among the 10 most downloaded models on huggingface, 9 are BERT-based and the remaining one is another transformer with around 33M parameters² In common benchmarks like DBPedia classification³, the top-three models are transformers with two of them also being variants of BERT. We chose our experimental setup to reflect this. Nevertheless, we are interested to see if SLALOM can provide useful insights for larger models as well and therefore experiment with larger models. To this end, we use a model from the BLOOM family [30] with 7.1B parameters as well as the recent Mamba model (2.8B) [21] on the Yelp-HAT dataset and compute SLALOM explanations. Note that the Mamba model does not even follow the transformer framework considered in this work. We otherwise follow the setup described in Figure 3 and assess whether our explanations can predict human attention. The results in Table 12 highlight that this is indeed the case, even for larger models. The ROC scores are in a range comparable to the ones obtained for the smaller models. For the non-transformer Mamba model we observe a drop in the value of the importance scores. This may suggest that value scores and linearized SLALOM scores are more reliable for large, non-transformer models.

²https://huggingface.co/models?pipeline_tag=text-classification&sort=downloads

³<https://paperswithcode.com/sota/text-classification-on-dbpedia>